section. This result is of course in accord with Margenau's Eqs. (23) and (24).[1]

At high densities, (19) reduces to the Maxwellian form

$$f_0 = N_0 \exp(-mv^2/2kT). \quad (22)$$

The transition from low to high densities is shown in Fig. 1. The mean energies and velocities at the three densities exhibited in Fig. 1 are given in Table I.

We next compute the effect of electron density on the conductivity when λ is constant. After eliminating f_1 and g_1 from (13) using (5), and making the approximation $\omega\lambda \gg v$, we find that the drift velocity $\bar{v}_z$ is given by

$$\bar{v}_z = \gamma/\omega[(4\bar{v}/3\omega\lambda)\cos\omega t + \sin\omega t],$$

showing that the in phase current is very much smaller than the out of phase current at these frequencies and pressures. The complex conductivity σ defined in (16) becomes

$$\sigma = (ne^2/m\omega)[(4\bar{v}/3\omega\lambda) + i] \doteq i(ne^2/m\omega).$$

This is identical with the result obtained for the constant τ case. The effect of varying density is here small, but of course can be readily estimated from the calculated values of $\bar{v}$ given in Table I.

In conclusion, it should be noted that whereas in the d.c. case, we noted a lowering of the entropy for increasing density, in the high frequency case, the drift velocity (in phase component) drops off with increasing density (see Table I) so that the same statement about entropy cannot be made. Since the out of phase component remains constant while the average velocity reduces for increasing density, the entropy is reduced to this extent.

PHYSICAL REVIEW VOLUME 75, NUMBER 5 MARCH 1, 1949

Ferromagnetism at Very High Frequencies
II. Method of Measurement and Processes of Magnetization*, **

M. H. JOHNSON AND G. T. RADO
Naval Research Laboratory, Washington 20, D. C.

(Received September 27, 1948)

A method for measuring the complex permeability, μ, of a ferromagnetic metal is described. The determination of both components of μ is accomplished by a simultaneous measurement of the changes in attenuation and phase velocity introduced into a conducting system by the ferromagnetism of one of its walls. An experimental technique involving pulsed magnetic fields is used. Values of μ for samples of magnetic iron at 200 and 975 Mc as a function of a polarizing magnetic field (which is parallel to the high frequency field) are compared to the static incremental permeabilities measured on the same sample. The interpretation of the experimental results indicates several characteristics of the magnetization in iron: the upper limit of domain dimensions in polarizing fields less than 500 oersteds is 10^{-4} cm; domains have different degrees of stability in the applied field; "weak-field domain" wall displacements are practically eliminated at the frequencies used; spin rotation and "strong-field domain" wall displacements are only slightly damped and contribute to the magnetization in weak as well as strong fields. Studies of hysteresis phenomena are discussed, and results on two types of permalloy presented.

I. INTRODUCTION

NUMEROUS investigations[1] have shown that two basic mechanisms are responsible for the changes in magnetization of a ferromagnetic substance placed in an external magnetic field. These mechanisms involve two different effects of the field on the configuration of the magnetically saturated regions, called domains,

* Paper I of this series, subtitled Magnetic Iron at 200 Mc, appeared in Phys. Rev. **71**, 322 (L) (1947). The method and its application to iron and permalloy at 200 Mc were briefly presented at American Physical Society meetings in January and April, 1947. Phys. Rev. **71**, 472 (Abstracts L4 and L5) (1947); Phys. Rev. **72**, 173 (A) (1947).

** It is a pleasure to acknowledge the invaluable assistance of Matthew Maloof in carrying out the experimental work described in the present paper.

[1] R. Becker and W. Doering, *Ferromagnetismus* (Verlagsbuchhandlung Julius Springer, Berlin, 1939).

which constitute the elements of the magnetic structure in a ferromagnetic specimen. In strong fields the magnetic moment of each domain turns from the axis of easy magnetization closest to the field toward the field direction, thereby producing the changes in magnetization. This mechanism is termed spin rotation or domain rotation. Its study, which must be made close to magnetic saturation, has led to a quantitative description of magnetization curves and thus to the evaluation of phenomenological constants for the anisotropic part of the crystalline energy. In weak fields most of the changes in magnetization are due to the growth of domains oriented favorably with respect to the field at the expense of less favorably oriented domains. This mechanism, termed wall displacement, involves the motion of a thin inter-domain boundary layer and is in itself rather involved. Although it has led to useful correlations, it has not, in general, yielded a quantitative theory of the magnetization curve.

There is no reason to expect that the two mechanisms will respond to rapidly changing fields in the same way. Consequently, the possibility arises that the study of magnetization at high frequencies might yield a more detailed understanding of each mechanism. Indeed, it will be shown that, if such a study is made in the presence of a polarizing field, certain domain sizes and dynamic characteristics can be derived from the experimental results. If these conclusions are substantiated by further experiments, the existing description of domains must be substantially modified.

High frequency ferromagnetic measurements in *metals* are difficult primarily because the conductivity severely limits the penetration depth of an electromagnetic wave. Consequently, only small effects on the wave propagation in an air space bounded by conductors can be produced by the permeability and resistivity of the metallic walls. We shall see in Section II that both the real and imaginary part of the propagation vector (attenuation and phase velocity) must be measured to determine the permeability of the metallic walls.[1a] While that portion of the attenuation which is caused by ferromagnetism is not difficult to determine, measurement of the corresponding change in phase velocity requires an exacting technique. One of the essentially new experimental features in the present work is the simultaneous measurement of both these changes when the latter are caused by the ferromagnetism of a metallic substance.

A simple substitution method suggests itself. If the ferromagnetic parts of a conducting system are replaced by a non-magnetic metal, the measured changes in the propagation vector suffice to determine the permeability of the replaced metal. By this means the attenuation can in fact be determined quite accurately. However, the changes in phase velocity, unlike the attenuation, can also arise from small changes in the geometry of the conducting walls and require that the substitution be made with a mechanical exactness that is difficult if not impossible to achieve.

In surmounting this difficulty we have used the results of work done at the M.I.T. Radiation Laboratory in 1942 under the direction of O. Halpern.[2] In some of the experimental arrangements there used, a polarizing field was applied *parallel* to the high frequency field. The large decrease in the attenuation thereby produced indicated that the high frequency permeability decreased in the manner predicted by the magnetization curve. Therefore, it should be possible to bring the high frequency permeability to unity by saturating the ferromagnetic metal. The substitution of a ferromagnetic by a non-magnetic conductor can thus be effected by a parallel magnetic field sufficiently strong to saturate the ferromagnet. Since no mechanical changes are made, the geometrical conditions can be maintained with the necessary precision.

Our experiments have been made in a coaxial line resonator tuned by a dieletric bead. The ferromagnetic sample constitutes a part of the center conductor. The calculation of the resonant frequency and Q for this cavity and the relation of these quantities to the permeability of the sample are the subjects of Section II.

[1a] In the work of Arkadiew, dating back to 1913 and summarized in J. Phys. USSR 9, 373 (1945), the necessity for measuring both resistive and reactive changes in order to determine the permeability is recognized. The experimental techniques used by Arkadiew are entirely different from those used by us and his work did not include a study of the effects of a superposed polarizing field.

[2] O. Halpern, Radiation Laboratory, M.I.T., Internal Report, Nov. 4, 1942. An account of these experiments is in preparation.

The polarizing field is generated by a direct current passing through the center conductor. Currents of the order of 1000 amperes are needed to saturate the sample. To avoid heating effects in the center conductor, a pulse technique must be employed. This technique and the associated ballistic indicator are discussed in Section III, together with the method of taking and interpreting the data.

Hysteresis effects can be rapidly examined in relatively small polarizing fields by using a low frequency polarizing current through the center conductor and putting the resonator output (after rectification and "chopping") on an oscilloscope. The resulting "butterfly curves" show the changes in attenuation as a function of cyclic polarization. This type of measurement is the subject of Section IV.

In Section V values of μ for samples of magnetic iron at 200 and 975 Mc as a function of a polarizing magnetic field (which is parallel to the high frequency field) are compared to the static incremental permeabilities measured on the same sample. The interpretation of the experimental results indicates several characteristics of the magnetization in iron: the upper limit of domain dimensions in polarizing fields less than 500 oersteds is 10^{-4} cm; domains have different degrees of stability in the applied field; "weak-field domain" wall displacements are practically eliminated at the frequencies used; spin rotation and "strong-field domain" wall displacements are only slightly damped and contribute to the magnetization in weak as well as strong fields. Studies of hysteresis phenomena are discussed, and results on two types of permalloy presented.

II. THEORY

Our first task (Part A) is to relate the propagation constant of an electromagnetic wave in a coaxial transmission line to the permeability, conductivity, and geometrical dimensions of the walls. Next we shall show (Part B) how changes in the propagation constant can be expressed by the change in Q and the change in resonance frequency of a coaxial line resonator. Finally (Part C) the complex permeability will be discussed, and formulas for its determination in terms of experimentally measurable quantities will be given.

A. The Propagation Constant

Consider an air-filled coaxial transmission line of circular cross section and choose cylindrical coordinates r, ϕ, and z such that the z direction coincides with the axis of symmetry. Let $r=a$ and $r=b$ be the radius of the inner and outer conductor, respectively. The metal walls (located at $r\leq a$ and $r\geq b$) will be characterized by a conductivity σ and a permeability μ.

We define the permeability[3] as the ratio B/H. In the case of time-dependent fields, μ must, in general, be assumed complex, so that **B** and **H** may be out of phase. This assumption simply means that there may exist a magnetic loss, in formal analogy with the dielectric loss of an insulator characterized by a complex dielectric constant.

The problem is to find a wave solution of Maxwell's equations which satisfies the boundary conditions at the metal walls and corresponds to the principal mode of propagation. In such a solution the non-vanishing components of the field are E_r, E_z, and H_ϕ. We shall make the following assumptions:

(1) The time variation of the field components is given by the factor $\exp(i\omega t)$, where the angular frequency $\omega=2\pi\nu$ is determined by the signal generator.

(2) The permeability $\mu=B/H$, as well as $\epsilon'=D/E$, the dielectric constant not due to conduction, are uniform and independent of the field components.

(3) Ohm's law is applicable and the density of free charge is zero.

(4) For metals, the apparent dielectric constant $\epsilon=\epsilon'-2i\sigma/\nu$ is given by $-2i\sigma/\nu$. For air, $\mu=1$, $\sigma=0$, and $\epsilon=\epsilon'=1$.

If k is the unknown propagation constant, and $k_0=2\pi/\lambda_0$ is the propagation constant in free space, Maxwell's equations in Gaussian units result in

$$H=(R/r)\exp(ikz), \tag{1}$$

$$E_r=-(k/k_0\epsilon)(R/r)\exp(ikz), \tag{2}$$

$$E_z=(ik_0\epsilon)^{-1}r^{-1}dR/dr\exp(ikz), \tag{3}$$

where the unknown function $R(r)$ is the solution of

$$rd/dr(r^{-1}dR/dr)-(k^2-k_0^2\epsilon\mu)R=0. \tag{4}$$

[3] In our experiment H is sufficiently small (≤ 0.01 oersted) to make μ independent of H. Hence we are dealing with a reversible (or "incremental") permeability, and the field equations are linear.

Since E_z/H must be continuous on the air metal boundary at $r=a$ and $r=b$, the above equations make it possible to calculate k.

In solving (4) for the metal walls, we choose a solution that corresponds to an attenuation of the field components with penetration into the metal. The calculation is simplified by the fact that σ is large so that $k_0(\epsilon\mu)^{\frac{1}{2}}\gg 1$ for all but very low frequencies. In solving (4) for the air space we make the approximation that $k-k_0$, which vanishes in the case of ideal walls ($\sigma=\infty$, $\mu=1$), is small compared to k_0 for sufficiently high frequencies.

The final expression for the propagation constant may be written

$$k=k_0(1-i\alpha+\beta), \tag{5}$$

where the real numbers α and β are defined by the relation

$$\alpha+i\beta=(2k_0\ln b/a)^{-1}\times[(1/a)(\mu_a/\epsilon_a)^{\frac{1}{2}}+(1/b)(\mu_b/\epsilon_b)^{\frac{1}{2}}], \tag{6}$$

and the subscripts on μ and ϵ identify the two conductors.

Equations (5) and (6) show that the necessary and sufficient condition for our approximation $[(k-k_0)/k_0\ll 1]$ to be valid is

$$(|\mu_a|)^{\frac{1}{2}}\ll(4\pi/c)(2\sigma\nu)^{\frac{1}{2}}a\ln b/a \tag{7}$$

with a similar condition for the outer conductor. In our experiment $a=0.159$ cm, $b/a=10$, and $\nu=2\times10^8$ sec.$^{-1}$, so that (7) becomes $(|\mu_a|)^{\frac{1}{2}}\ll 3.06\times10^{-6}\sigma^{\frac{1}{2}}$. For magnetic iron $\sigma\approx 8\times10^{16}$ sec.$^{-1}$ ($\sigma^{-1}=\rho\approx 11\times10^{-6}$ ohm-cm), and we find 100 to be a reasonable upper limit for $|\mu_a|$. These values lead to $(k-k_0)/k_0\approx 0.01$ and justify the approximation.

All three components of the electromagnetic field are seen to represent plane waves proportional to the factor

$$\exp[i(\omega t-kz)]=\exp(-k_0\alpha z)\exp[i\omega(t-z/v)],$$

where $v=c/(1+\beta)$ is the phase velocity of the waves in the transmission line. Evidently, α is a measure of the attenuation, and β is essentially the fractional deviation of the phase velocity from that in a transmission line with ideal walls.

Equation (6) shows that $\alpha=\beta$ if μ is real. Thus the permeability can be obtained either from an attenuation measurement or from a phase velocity determination. If, however, μ is complex, $\alpha\neq\beta$, and both α and β must be measured. Using the terminology of lumped electric circuits we may say that both the resistive and the reactive components of the impedance must be measured to determine the complex permeability. In general, α and β are of the same order of magnitude because $\mu\ll\epsilon$ in Eq. (6), but if μ is wholly imaginary, β is zero.

B. Resonant Frequency and Q

A half-wave resonant cavity is obtained by providing a coaxial line with metal end plates placed at $z=0$ and $z=l$, where $l\approx\lambda_0/2$. In calculating the Q of the resonator and the departure of its resonant frequency from c/λ_0 we shall assume ideal end plates (infinite σ and $\mu=1$) and use the values of the attenuation and phase velocity derived in part A. This procedure is justified by the fact that in our experiment, which is based on a substitution method, we are interested only in the effect of the imperfect inner conductor on the Q and resonant frequency. To find the actual Q and actual resonant frequency of the cavity, one would have to take into account the small, but measurable losses in the end plates.

In the case of perfectly reflecting end plates, the space variation of the electromagnetic field components is given by $A[\exp(ikz)-\exp(-ikz)]$, where the amplitude A is a known function of r. This expression satisfies the boundary conditions that it vanish at $z=0$, and it equal some fixed value p prescribed by the driving mechanism at $z=l$.

Since α is of the order of 10^{-3}, $k_0l\alpha\ll 1$, and we obtain, to a first approximation

$$|A|^2=(|p|^2/4)[(k_0l\alpha)^2\cos^2k_0l(1+\beta)+\sin^2k_0l(1+\beta)]^{-1} \tag{8}$$

as a measure of either the energy stored in the cavity or of the power dissipated during one cycle.

The cavity will resonate in its lowest mode if its length l is equal to $\lambda/2$, where $\lambda=\lambda_0/(1+\beta)$ is the wave-length in the resonator. This is equivalent to saying that for resonance the driving frequency ν must have a value such that

$$k_0l(1+\beta)=\pi, \tag{9}$$

which results in

$$|A|^2=|p|^2/4(k_0l\alpha)^2.$$

To reduce the energy in the resonator by one-half, the driving frequency must be changed by an amount $\Delta\nu$ which will make the denominator of Eq. (8) equal to $8(k_0l\alpha)^2$. This condition gives, to a first approximation, $(1+\beta)\Delta k_0=k_0\alpha$ so that $\nu/\Delta\nu=1/\alpha$.

For frequencies near resonance, Q is approximately constant ($Q\gg1$), and hence it may be defined by

$$Q=\nu/2\Delta\nu \tag{10}$$

which gives

$$\alpha=1/2Q \tag{11}$$

as the desired relation between α and that part of the Q which is due to the losses in the inner and outer conductor.

If $\Delta\nu'$ is the change in resonance frequency of the cavity compared to a similar cavity with ideal walls, we obtain from (9)

$$(\nu+\Delta\nu')l=c/2 \tag{12}$$

as the resonance condition for the case of ideal walls ($\beta=0$). Solving Eqs. (9) and (12) gives

$$\beta=\Delta\nu'/\nu \tag{13}$$

as the desired relation between β and that part of the resonance frequency shift $\Delta\nu'$ which is due to the losses in the inner and outer conductor.

Equations (11) and (13) lead to the following conclusions:

(1) Since β is positive, $\Delta\nu'>0$, so that the introduction of a loss decreases the resonance frequency of a cavity with ideal walls.

(2) The derivation of relations (11) and (13) merely assumes the existence of plane waves and of perfectly reflecting end plates. Thus, it is valid for certain modes in rectangular guides and other transmission lines.

(3) If we assume that all the walls of the coaxial resonator have a conductivity σ and a (real) permeability μ, Eqs. (6) and (11) lead to

$$Q=(4\pi/c)(\sigma\nu/\mu)^{\frac{1}{2}}(1/a+1/b)^{-1}\ln b/a. \tag{14}$$

Except for an additional term $[(8/\lambda_0)\ln b/a]$ in the denominator which arises from the losses in the end plates, Eq. (14) agrees with the well-known formula[4] for the Q of a half-wave coaxial resonator. If the permeability is complex ($\mu=\mu_1-i\mu_2$), our result shows that μ in Eq. (14) must be replaced by $|\mu|+\mu_2$, where $|\mu|=(\mu_1^2+\mu_2^2)^{\frac{1}{2}}$.

[4] See, for example, E. U. Condon, Rev. Mod. Phys. **14**, 341 (1942), Eq. (9¹16). Condon does not use the Gaussian units employed in the present paper.

C. The Complex Permeability

According to Eq. (6), α and β are proportional to the real and imaginary parts, respectively, of the quantity $(\mu/\epsilon)^{\frac{1}{2}}$, which itself is proportional to $(i\mu\rho)^{\frac{1}{2}}$. If we assume that the existence of a permeability $\mu\neq1$ gives rise to an energy loss in addition to the ohmic loss, then $\alpha>\beta$, and the permeability is seen to be represented by a complex number of the form $\mu=\mu_1-i\mu_2$. In certain cases (resonance, apparent diamagnetism), however, the permeability is not necessarily in the fourth quadrant.

It is now possible to derive the relations which allow the evaluation of the complex permeability, in any polarizing field, from measured values of changes in resonant frequency and Q.

If the ferromagnetic inner conductor of a coaxial line resonator is magnetically saturated, the change in the attenuation caused by the disappearance of the magnetic loss is given by $\alpha-\alpha_\infty$, where the symbol α now denotes the attenuation resulting from the inner conductor in a polarizing field H_0 and α_∞ is the value of α in a polarizing field sufficiently large to saturate magnetically the specimen under investigation. This method of reducing the permeability of the inner conductor to unity avoids the necessity for replacing the specimen by a non-magnetic metal and thus it surmounts the difficulties associated with changes in the geometrical configuration of the cavity. On account of Eq. (11), we may write

$$\alpha-\alpha_\infty=(1/2)(1/Q-1/Q_\infty), \tag{15}$$

where Q is the "Q" of the cavity in a polarizing field H_0, and Q_∞ is the value of Q in a saturating field.

Similarly, the disappearance of ferromagnetism as a result of the saturation causes a change in the fractional deviation of the phase velocity from the value c. Using Eq. (13), we can write

$$\beta-\beta_\infty=(\Delta\nu'-\Delta\nu_\infty')/\nu, \tag{16}$$

where β and β_∞ refer to the inner conductor, and $\Delta\nu'-\Delta\nu_\infty'$ is the change in resonance frequency of the cavity as the value of the polarizing field on the inner conductor is changed from H_0 to a saturating field.

The constant $\alpha_\infty=\beta_\infty$ may be calculated from Eq. (6) by setting $\mu=1$ and disregarding the con-

tribution of the outer conductor. Equations (15) and (16) make it possible, therefore, to obtain α and β in terms of measurable quantities. Using Eq. (6), μ_1 and μ_2 may then be evaluated for any H_0.

In practice it is more convenient to use a magnetic rod which is shorter than the inner conductor of the resonator. The remaining part of the inner conductor may be made out of a nonmagnetic rod (e.g., brass) having the same diameter as the test specimen. This procedure has the advantage that one can work with relatively high Q values throughout the experiment, and that the range over which the receiver and indicator must be linear can be reduced. If, on the other hand, the magnetic section of the inner conductor is too short, or if it is placed too near to the center of the resonator, then the magnetic effects are too small to be measured accurately. It was found that a satisfactory compromise is obtained by making the specimen long enough to prevent end-effect errors[5] and placing it in such a position[5] that Q_∞/Q is never larger than about two or three.

By solving the appropriate boundary value problem,[5] the effect of the partially magnetic inner conductor can be predicted with sufficient accuracy. It is shown in Appendix I that the use of a magnetic section (instead of a completely magnetic inner conductor) reduces the magnetic effects $\alpha-\alpha_\infty$ and $\beta-\beta_\infty$ by a factor γ, the value of which is between zero and unity and depends exclusively on the frequency, the length of the specimen, and its position with respect to the center of the resonator.

The problem of measuring Q for large values of H_0 introduces additional difficulties. As the polarizing field H_0 has to be parallel to the high frequency magnetic field, H_0 must be generated by passing a large current through the inner conductor. To avoid excessive heating, this current and hence H_0 must be pulsed. Consequently the quantity Q can be measured directly only for small[6] values of H_0. For other values of H_0, and particularly for saturating fields, only Q ratios can be measured. If, however, the Q in zero polarizing field is chosen as the reference value, the Q ratios are found to be irreproducible because of the hysteresis effects discussed in Section IV. For this reason we have used as the reference value the $Q=Q_{\text{bias}}$ measured in a "biasing" field $(H_0)_{\text{bias}}$ which, without being too large to prevent continuous application, is yet large enough to minimize hysteresis effects. In the case of magnetic iron $(H_0)_{\text{bias}}=6.25$ oersteds was used. This value corresponds to an abscissa beyond the knee of the static magnetization curve.

On the basis of the above modifications, we can write Eqs. (15) and (16) in their final form.

Using the abbreviations

$$Q/Q_{\text{bias}}=\chi \quad \text{and} \quad Q_\infty/Q_{\text{bias}}=\chi_\infty,$$

we obtain from Eq. (15)

$$\alpha-\alpha_\infty=(2\gamma\chi_\infty Q_{\text{bias}})^{-1}[(\chi_\infty/\chi)-1]. \quad (17)$$

Using the abbreviations

$$\Delta\nu'-\Delta\nu'_{\text{bias}}=\delta \quad \text{and} \quad \Delta\nu'_\infty-\Delta\nu'_{\text{bias}}=\delta_\infty,$$

we obtain from Eq. (16)

$$\beta-\beta_\infty=(1/\gamma\nu)(\delta-\delta_\infty), \quad (18)$$

where δ is the change in resonance frequency of the cavity as the value of the polarizing field on the inner conductor is changed from H_0 to $(H_0)_{\text{bias}}$, and δ_∞ is the value of δ if H_0 is a saturating field.

Using $\mu=1$ in Eq. (6) and disregarding the contribution of the outer conductor, we obtain

$$\alpha_\infty=\beta_\infty=(c/8\pi)(\rho/\nu)^{\frac{1}{2}}/a\,\ln(b/a), \quad (19)$$

where $\rho=1/\sigma$ is the resistivity of the magnetic specimen in electrostatic units (seconds).

As shown in Appendix I, γ may be calculated from the formula

$$\gamma=(1/\pi)[k_0L+(2\sin^2k_0D-1)\sin k_0L], \quad (20)$$

where L is the length of the magnetic specimen, D is the distance of its center from the center of the resonator, and k_0, as before, is equal to $2\pi\nu/c$.

Using $\mu=\mu_1-i\mu_2$ in Eq. (6) and disregarding the contribution of the outer conductor, we arrive at the final relations

$$\mu_1=\alpha\beta/\alpha_\infty^2, \quad (21)$$

$$\mu_2=(\alpha^2-\beta^2)/2\alpha_\infty^2 \quad (22)$$

[5] See Appendix I.

[6] In our resonator, fields up to about 6 oersteds, corresponding to about 5 amperes, can be applied continuously.

for the determination of the complex permeability.

The quantities Q_{bias}, ρ, and ν are easily measured by standard methods. Thus, the important part of our experiment consists in measuring simultaneously χ and δ as a function of H_0 by the special technique described in Section IIIB. In principle, χ_∞ and δ_∞ may also be measured by this technique. For practical reasons (see Section III), however, these quantities are sometimes obtained by extrapolating[7] the χ and δ curves to infinite fields. Equations (17) through (22) may then be used to calculate $\mu=\mu_1-i\mu_2$ for any value of H_0.

III. EXPERIMENTAL

Figure 1 shows a cross-sectional view of the coaxial cavity and a block diagram of the principal components of the apparatus.

A. Measurement of Q_{bias}

(1) *Apparatus*

In principle, Q-values were determined by measuring the voltage transmitted by the cavity as a function of frequency, and calculating the Q from several points on the resonance curve.

To obtain the required accuracy, however, it was found preferable to use a fixed frequency and to change the resonant wave-length of the cavity by means of a dielectric bead. Thus the R. F. oscillator could be left undisturbed for extended periods of time, resulting in increased frequency stability and constancy of power output. If, as in our case, the calibration of the bead (position *versus* frequency) is theoretically linear, then differences in "frequency" (actually differences in resonant wave-length) can be measured with a fractional error ($<10^{-5}$) smaller than that of commercially available crystal-calibrated heterodyne frequency meters ($\geq 10^{-4}$).

The coaxial resonator is approximately one-half wave-length long (74.5 cm) at 200 Mc and is shorted at both ends. The radii ($a=0.159$ cm, $b=1.59$ cm) were chosen so as to satisfy the following requirements: (1) Most of the resonator losses should take place in the inner conductor; (2) the radius of the inner conductor should be sufficiently large compared to the skin depth, a requirement contained in Eq. (7); (3) ferromagnetic rods having the diameter of the inner conductor should be available; (4) the Q of the cavity should be in a convenient range ($\sim$500 to 1000).

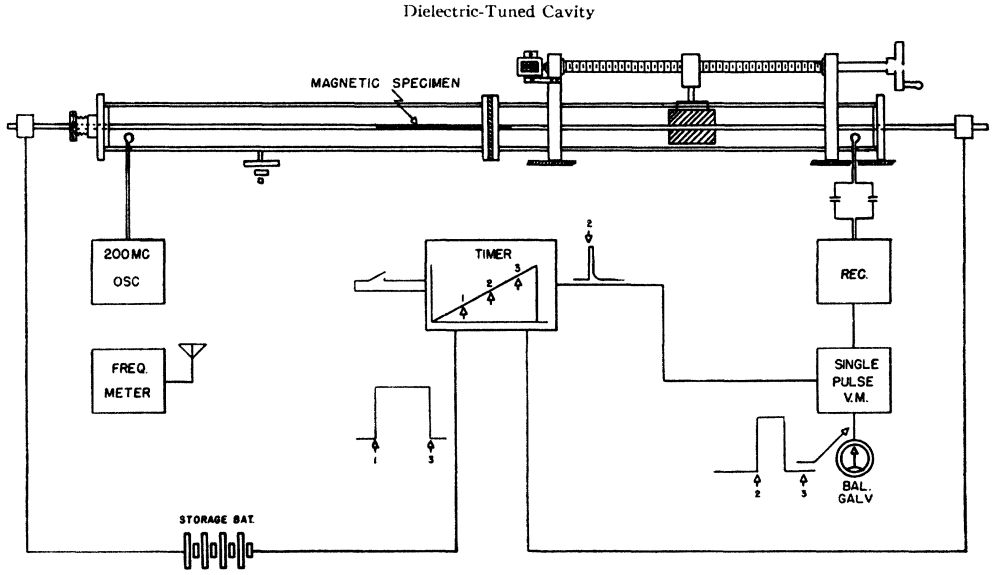

FIG. 1. Cross-sectional view of the coaxial cavity and block diagram of the principal components of the apparatus.

[7] For soft magnetic materials the fields at our disposal permitted a very close approach to saturation. Hence, the extrapolation was fairly accurate (see paper I and Section V of the present paper), especially since χ_∞ can be calculated in terms of (1) the measurable Q of a similar resonator whose center conductor is brass, and (2) the known conductivities of the magnetic specimen and brass. This calculation is presented in Appendix II.

Except for the outer conductor, which is made of copper,[8] brass is used throughout the construction of the cavity. A thin mica washer, located at the center of the cavity, prevents the polarizing current from flowing through the outer conductor. The magnetic specimen, whose diameter is that of the inner conductor, has a well-defined[9] length of 17.75 cm, and its center is located at the proper distance (two to four inches) from the center of the resonator to produce a γ-factor of the desired magnitude.[5] The inner conductor is held in the end plates of the cavity by means of set screws. In order to prevent sagging of the inner conductor it is put under a small tension (with the use of an appropriate screw arrangement) before one of the screws is tightened. This tension is approximately 0.6 kg/mm^2 and does not affect the value of Q.

Tuning of the cavity is accomplished by displacing a polystyrene bead along the axis of the cavity. The cylindrical bead (3 cm long) was attached to a rider on a calibrated screw (26 threads/in.) and its size was such that it filled the space between the inner and outer conductor without actually touching them. A sufficiently linear calibration curve of "counter units" (i.e., number of rotations of the calibrated screw) *versus* frequency is obtained by centering the motion of the bead around the $\frac{1}{4}$-length point of the cavity (see Appendix III). The deviations from linearity and the reproducibility of the calibration are smaller than one percent. A Cardwell crystal-calibrated frequency meter was used in these measurements.

The source of R. F. power is a resonant line oscillator using a 2C39 tube and working as a Hartley circuit. In order to keep the frequency constant to 0.001 percent, and the power output to 1 percent, it was found necessary to keep the output down to about 30 milliwatts.

The receiver is a standard APR-1 superheterodyne which was suitably modified to improve its stability and the linearity of its output/input voltage ratio. Output values are read on a 0–100-d.c. microammeter in series with the second detector. The remaining non-linearity (one or two percent) was corrected for by calibrating the receiver in terms of the attenuator on a type LAF-1 signal generator.

TABLE I. Typical Q-measurement. Data of 1/10/47, taken (at 200 Mc) on a 17.75-cm rod of magnetic iron whose center was at a distance of four inches from the electrical center of the cavity. The readings R and R_{res} (see text) of the output meter in microamperes are corrected for the zero-signal diode current (2.7 microamperes in this case) and for the small non-linearity of the receiver. In the first row of the table, for example, the uncorrected readings of R and R_{res} were 80.0 and 88.8, respectively. C_R and C_R' are the counter readings at two equal output readings R. The center of the resonance curve is at $(1/2)(C_R+C_R')$, and $2\Delta C$, its width at the level R, is given by $C_R'-C_R$.

R	R_{res}	C_R	C_R'	C_R+C_R'	$2\Delta C$	$q\times10^3$
77.3	86.1	427	569	996	142	3.47
67.2	85.4	387	612	999	225	3.48
56.9	85.4	336	659	995	323	3.47
47.1	85.6	279	714	993	435	3.49
37.3	85.5	200	792	992	592	3.49

Average value of $(1/2)(C_R+C_R')=497.5\pm1$ counter units.
Average value of $q\times10^3=3.48\pm0.01$ (counter units)$^{-1}$.
$Q=\nu sq=2\times10^5\times0.520\times3.48\times10^{-3}=362$.
Frequency error $\doteq\pm1$ counter unit $\doteq\pm2$ kc $\doteq0.001$ percent of ν.

(2) *Procedure*

By a suitable arrangement of the input and output coupling loops of the cavity, a considerable transmission loss (60 db) was introduced between the oscillator and receiver. Thus, the decoupling was sufficient to regard the measured Q's as unloaded Q's: a change of 12 db in the coupling changed the Q by less than 1 percent.

From the standard formula of the resonance curve, the expression

$$Q=(\nu s/2\Delta C)[(R_{res}/R)^2-1]^{\frac{1}{2}}=\nu sq \qquad (23)$$

is easily derived. Here ν is the frequency (2×10^5 kc), s the calibration constant of the cavity (approximately 0.52 counter unit/kc), R_{res} the reading of the output meter when the cavity is at resonance, and $2\Delta C$ the width of the resonance curve, in counter units, between two equal output readings R. The values of R_{max} and R are corrected for the small non-linearity of the receiver.

Using four or five pairs of points on the resonance curve extending down to the $\frac{1}{4}$-voltage point, the various Q values agreed occasionally

[8] The type of metal used for the various parts of the cavity was determined by its availability in the proper shape. The calculations were corrected for the different resistivity of the inner and outer conductor.

[9] The difference in diameter of the brass inner conductor and of the threaded portions (≈1 cm long) on both ends of the specimen is much larger than the skin depth in brass.

to ± 0.2 percent and always to ± 0.5 percent. Table I presents a typical example of a Q-measurement. If the inner conductor were removed from the cavity and then replaced, Q could be reproduced, over a period of several months, to better than 1 percent in the case of a brass inner conductor and to about 2 percent in the case of a partially magnetic inner conductor. The latter error is due to a hitherto unexplained magnetic effect which appears to be connected with hysteresis and often manifests itself as a slow change of the magnetic state over a period of about a day.

To obtain Q_{bias}, a constant current of 5.0 amperes was passed through the partially magnetic inner conductor. With this current flowing, the sample was demagnetized by superposing a 60-cycle a.c. on the biasing current and gradually (in approximately 3 seconds) decreasing its magnitude from a maximum value of 45 amperes RMS with the help of a variac. $Q = Q_{\text{bias}}$ was then measured as described above.

The gradual 2 percent variation of the Q with time could often be reduced, but not always eliminated, by pulsing the cavity at the beginning of a series of measurements several times with a field of about 1000 oersteds and demagnetizing between pulses.

An experimental test of the combined error resulting from the frequency instability of the oscillator and the mechanical error of the tuning mechanism presents itself in the reproducibility of the center of the resonance curve on the counter units scale. Since the center of the resonance curve, as determined by the arithmetic mean of the counter readings at two equal R values, could be reproduced to one counter unit (see Table 1), the over-all frequency error of the apparatus is, as already mentioned, about 0.001 percent.

The experimental Q values for the cavity with brass inner conductor were consistently lower, by about 8 percent, than that calculated ($Q = 685$) by Eq. (14) with the additional term in the denominator which arises from the losses in the end plates. Except for σ, which was measured on the inner conductor, but not on the outer conductor or on the end pieces, the parameters in this calculation are well-known. Since about 80 percent of the losses occur in the inner conductor, the theoretical Q cannot be in error by 8 percent.

As errors caused by coupling were eliminated (<1 percent), and as no radiation losses could be detected, we conclude that the "Q deficit" is due to unknown losses in the resonator. Imperfect contacts at the junctures of the inner conductor and the end pieces of the cavity appear to be the most probable locations of these losses. Since the measured Q's are reproducible, however, they may be used for the calculation of Q_∞ (see Appendix II) and no errors arise from the existence of the "Q deficit."

The validity of our permeability measurements may be questioned, of course, if our failure to realize experimentally the calculated Q is due to the non-applicability of measured σ[10] values to the surface layer of metals. Since some simple experiments (non-metallographic polishing of the surface of the inner conductor, soft soldering of the inner-conductor to the end-plate joints) did not increase the Q, the matter was not investigated further even though the limited literature on this problem appears to contain inconsistent results. As the theoretical value of Q_∞, which depends on σ (see Appendix II), was checked experimentally, and as some of the final results (the equality of μ_{stat} and μ_1 for iron over a large range of H_0) are so readily interpretable, it was assumed that no anomalies in σ exist. It should be stated, however, that in the case of 45 Permalloy (the extrapolated) experimental value of Q_∞ is 3 percent smaller than the calculated value.

B. Measurement of χ and δ

(1) *Apparatus*

The quantities χ and δ were determined by measuring, with two values (H_0 and $(H_0)_{\text{bias}}$) of an applied polarizing field, the voltage transmission of the cavity as a function of resonant wave-length. From the ratio of the two resonance

[10] The results of the well-known Hagen-Rubens experiment make it appear extremely unlikely that the value of σ at UHF differs from the static value.
The variation of σ with a magnetic field (magneto-resistive effect) should, in principle, be taken into account. For the substances used in our investigation, however, this effect is about ten times too small to cause noticeable errors.

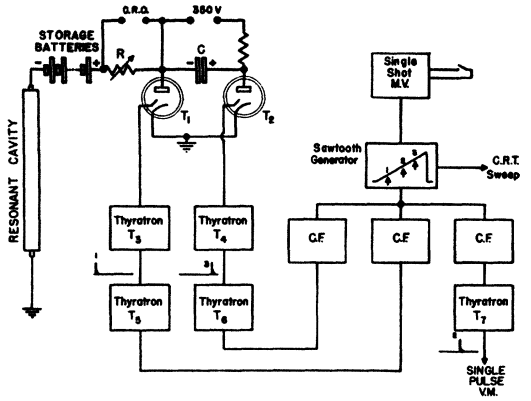

FIG. 2. Schematic diagram of the 1000-ampere pulser and block diagram of the timing circuit. The tubes T_1 and T_2 are ignitrons (GL-415).

curves thus obtained (see inset, Fig. 3), χ and δ are easily calculated.

The purpose of the circuits to be described is twofold. First, a direct current (i.e., the polarizing current which generates H_0) must be applied to the inner conductor for a short time interval Δt_p. Second, the high frequency transmission of the cavity must be measured during an interval Δt_v located within Δt_p, and during an equal interval $\Delta t_v'$ located outside of Δt_p.

In order to eliminate errors caused by the transient skin effect, it is obviously necessary for H_0 to be constant (or at least to have penetrated into the inner conductor a distance of several skin depths) at the time the "viewing pulse" measures the high frequency transmission of the cavity. By observing the shape of the current pulses on an oscilloscope it was found that the inductive transients die out in about one[11] millisecond. Nevertheless, a pulse length Δt_p of about 8 milliseconds was adopted in all measurements. This arrangement made it possible to "move" Δt_v within Δt_p, and thus it provided a means of checking on the flatness of the top of the current pulses by comparing measurements of the cavity transmission at different times within Δt_p. The same technique was used and found to be invaluable in investigating heating effects. It was shown that even in the highest fields the transmission is independent of the viewing time if the front edge of Δt_v is moved between the limits of 1 msec. and 5 msec. from the beginning of Δt_p.

To obtain reproducible data in spite of the hysteresis effect, it proved necessary to demagnetize the sample after every current pulse before the "unpulsed transmission" could be measured during the interval $\Delta t_v'$. The heating of the inner conductor as a result of the combined effect of the demagnetizing a.c. and the high current pulse necessitated a waiting period of $\frac{1}{2}$ to 3 minutes between the Δt_p pulses. It is evident, therefore, that a system employing regularly repeated pulses would not have any advantages over the "single pulse system" (SPS) adopted here.

Figure 1 shows the general function of the circuits. Between the instants denoted by "1" and "3" a current pulse Δt_p is applied to the inner conductor of the cavity. At the instant denoted by "2" a trigger activates the single pulse voltmeter (SPVM) which measures the transmission of the cavity during the viewing pulse Δt_v starting at "2."

Figure 2 shows a more detailed schematic diagram of the pulser and a block diagram of the timing circuit. The high currents are obtained from 14 low resistance storage batteries (Navy Type No. 17-B-9536) connected in series.[12] The pulses are started and stopped by firing the ignitrons T_1 and T_2, respectively. Tube T_1 (the "starter") is turned off at the end of Δt_p by applying to its plate a negative pulse from the large (3200-μf) condenser through tube T_2, the latter being extinguished automatically as the condenser discharges. The magnitude of the current pulses is controlled by means of an appropriate series resistor R. For low currents, commercially available non-inductive resistors of high wattage are used. For high currents, the resistors were made of manganin wire. The size of the voltage pulse across R, as determined on a calibrated cathode-ray oscilloscope with a long persistence screen (Type P7), provides a measurement of the polarizing current with an accuracy of ± 2 percent. For the cavity described in this

[11] A rigorous theoretical solution of this transient problem is hardly possible as the permeability is unknown. Furthermore, the field equations become non-linear since the effective permeability to the applied square wave field depends (in an unknown manner) on H_0. By assuming a constant permeability of 1000 (upper limit), however, a penetration time of the order of milliseconds was calculated.

[12] In view of the relatively long duration of Δt_p and the requirement of reasonably flat pulses, the use of a condenser would involve prohibitively large capacities. The problem of pulsing a generator was not explored.

paper, the value of H_0 on the surface of the inner conductor ($2i/10a$) is $1.25i$, where i is the polarizing current in amperes.

The timing circuit is largely conventional. By adjusting the bias on the three 2050 thyratrons it is possible to vary the length of Δt_p, its position on the linear sweep, and the starting time of the viewing pulse Δt_v. The length of Δt_v (2 milliseconds) is also adjustable and is determined by the time constant of a one-shot multivibrator which is a part of the single pulse voltmeter (SPVM).

To determine the transmission of the cavity during Δt_v, one might measure the output pulse of the receiver (i.e., the voltage drop across the load resistance of the second detector) on an oscilloscope. This method, however, does not have the required precision (<0.5 percent) during a single pulse. Instead, we developed the SPVM, which consists of a pulsed cathode follower bridge in conjunction with a ballistic galvanometer[13] and measures ballistically the output current of the receiver during Δt_v. Since the pulses are flat and Δt_v is constant, the galvanometer deflection is proportional to the receiver output.

The apparatus described here has been operating satisfactorily since September, 1946. Among the important practical problems that were encountered are the elimination of interference (the cavity and receiver were situated in separate screen rooms) and the minimizing of pick-up due to the large pulse currents by properly locating the ground points.

(2) *Procedure*

The transmission V_{bias} of the cavity in the biasing field ($(H_0)_{\text{bias}}=6.25$ oersteds is continuously applied to the inner conductor) is measured on the SPVM by disconnecting the igniters of T_1

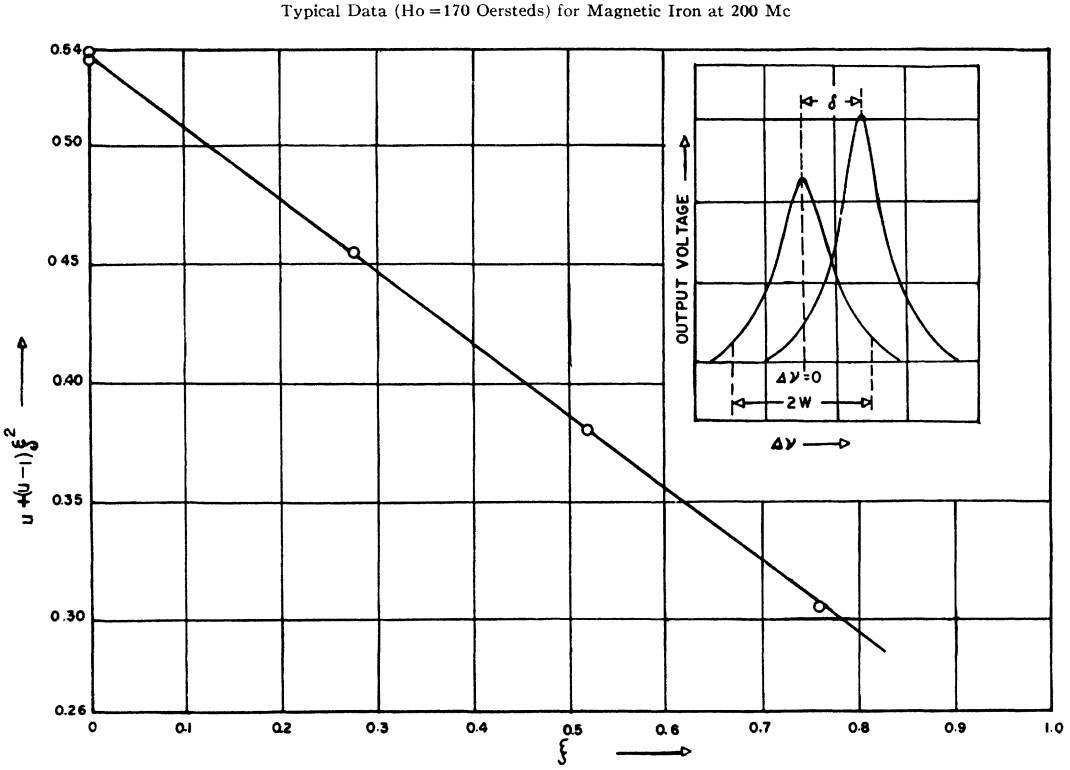

FIG. 3. Typical experimental curve used for the determination of χ and δ at a given polarizing field and frequency. Inset: Schematic representation of resonance curves for $(H_0)_{\text{bias}}$ (left), and H_0 (right), illustrating the increased Q and increased resonant frequency obtained by pulsing the cavity.

[13] G. T. Rado, M. H. Johnson, and M. Maloof, "A single pulse voltmeter," paper to be submitted to The Review of Scientific Instruments.

and T_2 from the circuit. About $\frac{3}{4}$ minute later (the period of the galvanometer is about 30 seconds) the cavity is "pulsed," and the transmission V corresponding to H_0 is measured. Then the sample is demagnetized, and after it has cooled off, both V_{bias} and V are checked twice. Starting from the center of the "unpulsed" resonance curve (corresponding to $(H_0)_{\text{bias}}$), the ratio $u=(V_{\text{bias}}/V)^2$ is measured at various counter settings, i.e., various resonant wave-lengths. The

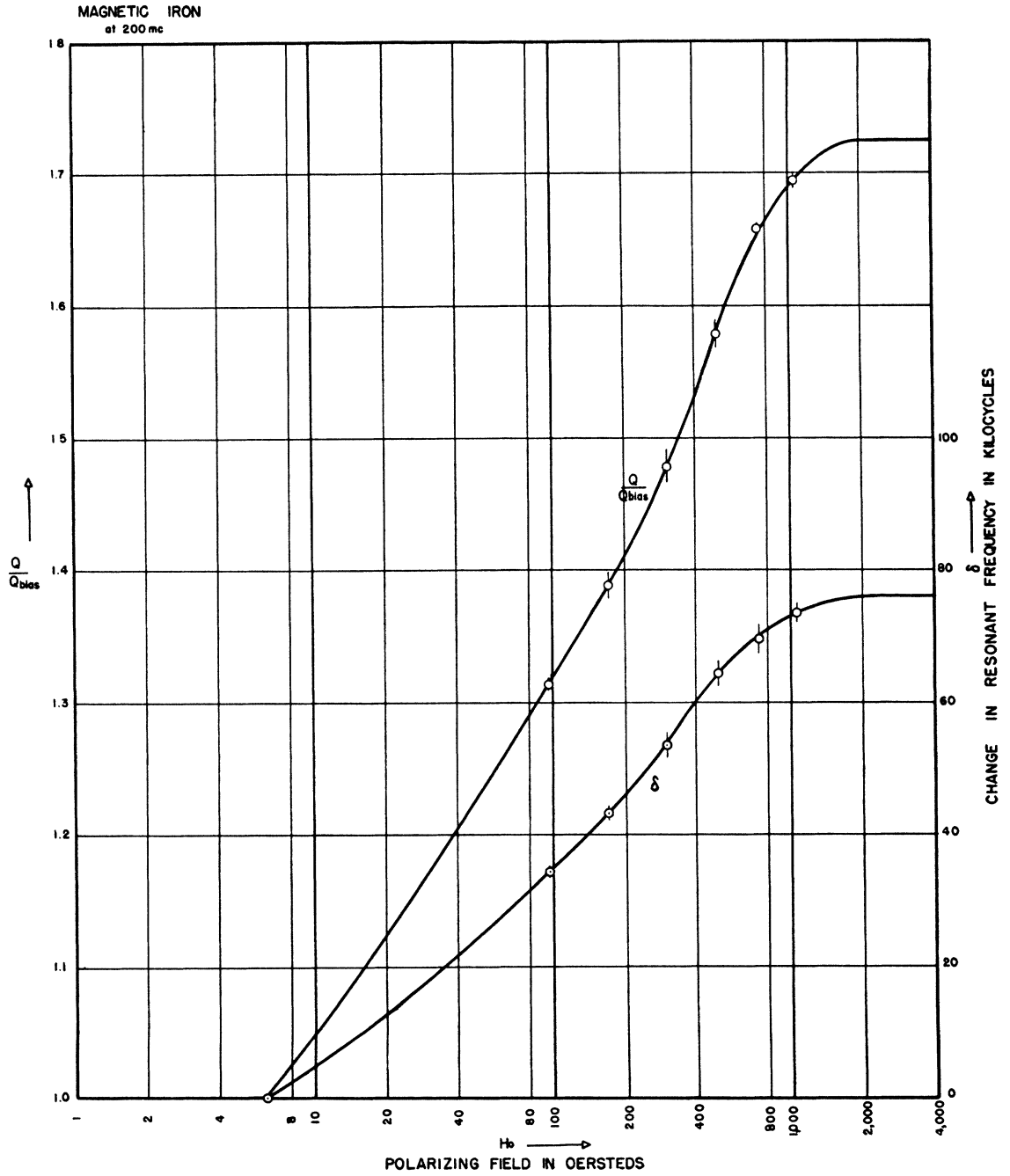

FIG. 4. Q ratio and change in resonant frequency as a function of the polarizing field H_0 for magnetic iron at 200 Mc.

values of χ and δ for any given H_0 are determined as follows:

From the standard formula of the resonance curve one obtains

$$(V_{\text{bias}}/V)^2=(V_{\text{bias}}'/V')^2 \times[1+4Q^2(\delta-\Delta\nu)^2/(\nu+\delta)^2] \times[1+4Q_{\text{bias}}^2(\Delta\nu/\nu)^2]^{-1}, \quad (24)$$

where $\Delta\nu$ is the change in resonance frequency measured from the center ν of the unpulsed resonance curve, and the primed quantities denote maximum (i.e., resonant) values. On the basis of Section II, the shift δ in Eq. (24) must clearly be positive: the center $(\nu+\delta)$ of the pulsed resonance curve (which corresponds to relatively small magnetic losses) must occur at a higher frequency than the center of the unpulsed resonance curve (which corresponds to relatively large magnetic losses).

Since $\delta\ll\nu$, and since for a decoupled resonator $V_{\text{bias}}'/V'=Q_{\text{bias}}/Q$, Eq. (24) may be rearranged to yield

$$u+(u-1)\xi^2=\chi^{-2}+(\delta/W)^2-(2\delta/W)\xi, \quad (25)$$

where $\xi=\Delta\nu/W$, and $2W=\nu/Q_{\text{bias}}$ is the width of the unpulsed resonance curve at the half-power point.

Plotting the measured quantity $u+(u-1)\xi^2$ as a function of the measured quantity ξ, one obtains a straight line whose slope and intercept furnish δ and χ, respectively. Figure 3 is an example of such a graph. It is seen that the slope of the straight line is negative so that δ is positive, as expected.

In practice, of course, the frequency is held constant and the resonant wave-length changed by varying the position of the dielectric bead. Expressing all the frequencies in counter units, we obtain the expressions[14] $W=1/2q_{\text{bias}}$ and $\xi=-(\Delta C)2q_{\text{bias}}$ which involve only directly measurable quantities. As the terms of Eq. (25) are dimensionless, we obtain

$$\delta=(\text{slope})W/2s \text{ kilocycles}, \quad (26)$$

and

$$\chi=[\text{intercept}-(\text{slope}/2)^2]^{-\frac{1}{2}}, \quad (27)$$

where s and q were defined in connection with Eq. (23), and q_{bias} is the value of q for $H_0=(H_0)_{\text{bias}}$.

If the response of the apparatus were perfectly linear, $u=(V_{\text{bias}}/V)^2$ would be given by $(G_{\text{bias}}/G)^2$, where G and G_{bias} are the galvanometer deflections corresponding to the voltage transmissions V and V_{bias}. Actually the combined errors resulting from the small non-linearity of the receiver and the SPVM, as well as from the flat scale on the galvanometer, happen to lead to a rather accurate proportionality between the deflections and the ηth power of the voltage. Thus $u=(G_{\text{bias}}/G)^{2/\eta}$, where the value of $\eta(\approx 1.02)$ is determined by an over-all calibration of the system with an R.F. signal generator.

The procedure described above leads to experimental curves of χ and δ *versus* H_0. Typical results of this kind (magnetic iron at 200 Mc) are given in Fig. 4. The saturation values χ_∞ and δ_∞ are obtained either experimentally, as in the case of 4–79 Mo-Permalloy, or by extrapolation to infinite fields, as in the case of magnetic iron. As stated in paper I, χ_∞ can be calculated (see Appendix II), and thus it is much more accurately determined than δ_∞, which must be found by a measurement or an extrapolation that cannot be verified.

C. Static Measurements and Preparation of Specimens

The static incremental permeabilities were measured by Mr. E. A. Gaugler of the Naval Ordnance Laboratory on the identical specimens used for the 200-Mc tests. These samples are $\frac{1}{8}$-inch diameter rods having a length of 17.75 cm (plus threads) and an effective axial ratio of 57. A longitudinal magnetizing field was produced in an oil-cooled solenoid coaxial with the specimen. The demagnetization correction was based on Bozorth and Chapin's[15] tabulation of the demagnetizing factor of rods as a function of the apparent static permeability and the axial ratio. Both the induction and its increment were

[14] Since the correct sign determination for δ is rather important, it seems appropriate to mention that the minus sign in the expression for ξ is not erroneous even though the cavity is constructed in such a manner that a displacement of the dielectric bead away from the center of the cavity, which causes an increase in the cavity's resonance frequency, happens to be accompanied by an increase in the counter reading. The minus sign results from the fact that we obtain what is in effect a positive $\Delta\nu$ not by increasing the applied frequency, which is actually constant, but by decreasing the counter reading and thus decreasing the resonance frequency of the cavity.

[15] R. M. Bozorth and D. M. Chapin, J. App. Phys. **13**, 320 (1942).

measured ballistically. The thin search coil was placed near the center[15] of the rod and the correction for the flux in the air space was obtained experimentally. Since the incremental changes of the magnetic field were sufficiently small, their magnitude did not affect the measurements of μ_{stat}. With the exception of the early part of the magnetization curve, where the demagnetization correction is somewhat uncertain, Gaugler's values of μ_{stat} are at least as accurate as our high frequency permeabilities. Fortunately, however, the exact value of the large static incremental permeabilities at very small polarizing fields is of little interest (Section V) for our purposes. In the coaxial line measurements, of course, the demagnetizing field is zero for both the static and the high frequency lines of force. The static measurements refer to the initial magnetization curve rather than to the particular method of traversing the magnetization curve used in the high frequency case. At polarizing fields of several oersteds the difference between these two procedures has a negligible effect on μ_{stat}.

All specimens were made from rods[16] that had been annealed before we received them. The process of threading the samples did not significantly change their magnetic properties. This conclusion was reached by re-annealing the iron specimen (in an H_2 atmosphere at 1100°C) after the static and 200 Mc measurements were completed, and then re-measuring μ_{stat}. The results agreed with the original static measurements even at small polarizing fields where the effect of any appreciable stresses would be most pronounced. Since the static results could be reproduced on two specimens of equal length made from adjacent portions of the iron rod, it was unnecessary to attempt static measurements on the short (4-cm) specimen, used for our 975 Mc[17] work, which was cut from the original rod. In the case of the permalloys the above mentioned verifications were omitted so that residual stresses due to the threading may have caused μ_{stat} to be too low in the relatively unimportant region of small polarizing fields. For large values of H_0, however, the static results are in satis-

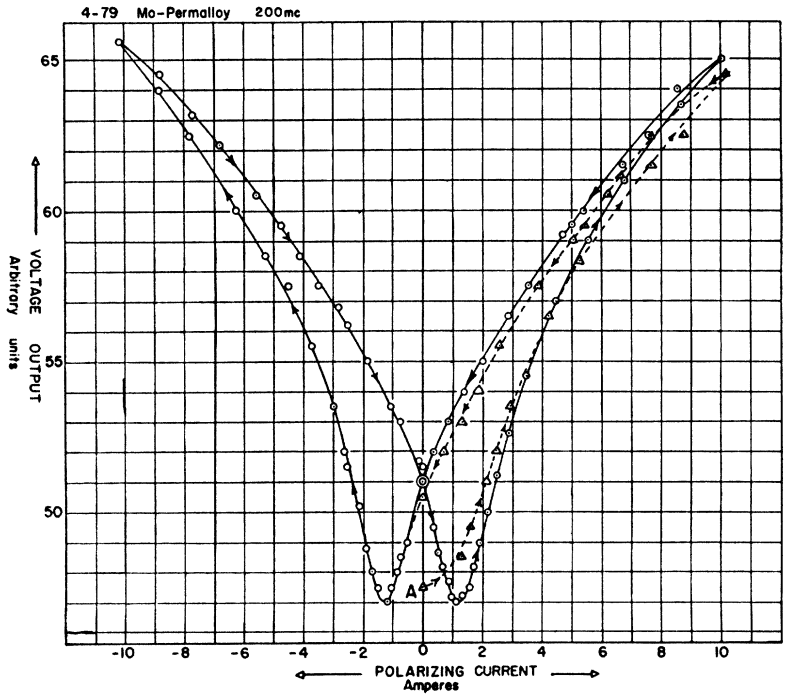

FIG. 5. Typical butterfly curve (4–79 Mo Permalloy at 200 Mc) obtained by using a d.c. polarizing current. The starting point (marked "A") represents the demagnetized state.

[16] We are indebted to Mr. R. A. Chegwidden of the Bell Telephone Laboratories for samples of the magnetic materials used in this work.

[17] The 975-Mc measurements were made in a special resonator by a method practically identical with the one described in the present paper. We wish to thank Mr. H. Rosenblatt for his help in taking some of the data. Further results, including the effect of surface treatments on the complex permeability, will be reported in a later publication.

TABLE II. Summary of butterfly data.

I	II	III	IV	V	VI
Material	ν in Mc	H_0 at max μ	μ_0	μ/μ_0 at $H_0=18$ oersteds	μ/μ_0 at max μ
Iron	0	1.0	55 (198)	0.5	2.5
	200	2.7	95	0.68	1.10
	975	3.5	66	0.87	1.01
Mo Permalloy	0	0.05	7,000 (11,700)	$\sim 10^{-4}$	1.5
	200	2.2	64	0.41	1.32
45 Permalloy	0	0.3	1,200 (2,700)	0.06	1.9
	200	~ 4.0	81	0.87	1.03

Column I: The materials used by Elmen (see reference 22) for his static measurements were Armco iron, 3.8–78.5 Mo Permalloy, and 45 Permalloy, whereas the high frequency results refer, of course, to magnetic iron, 4–79 Mo Permalloy, and 45 Permalloy. Any comparison of the static and high frequency data of this table must thus be qualitative. Only the data of Figs. 9, 11, and 12 may be used for a quantitative comparison of static and high frequency results.

Column II: The data quoted for $\nu=0$ are Elmen's (see reference 22) results at 200 cycles/sec. Presumably these data apply to the static case.

Columns III–VI: At the high frequencies, the permeabilities listed in these columns are apparent permeabilities (μ_R) and were measured (Section IV) by the brass substitution method in conjunction with the butterfly technique. At zero frequency the permeabilities are static incremental permeabilities (μ_{stat}). In either case the subscript zero indicates that $H_0=0$. Except for the data in parentheses, which refer to the demagnetized state, all values of μ_0 (including those in the ratios of columns V and VI) refer to the cross-over point of the butterfly and are thus characteristic of remanence. The high frequency results were obtained from butterfly curves whose maximum value of H_0 was taken as 17.7 oersteds in the case of magnetic iron and 4–79 Mo Permalloy, and as 35.4 oersteds in the case of 45 Permalloy.

factory agreement with representative values published by Legg.[18]

The surface of each specimen is reasonably smooth, only a few fine ridges in the direction of the axis being visible to the unaided eye. Microscopic examination revealed additional irregular striations and pitted regions.

The purity of our magnetic iron is listed as 99.94 percent, and a spectrochemical analysis at this laboratory showed that the metallic impurities total less than 0.03 percent. It seems reasonable to assume, therefore, that the accepted value[1] of the anisotropy constant of iron agrees closely with that of our particular material. The pertinent conclusions of Section V remain valid as long as the discrepancy between these two values does not exceed a factor of three.

IV. HYSTERESIS EFFECTS

The measured quantities Q_{bias}, χ, and δ, and hence the high frequency permeability, were found to be independent of the R. F. field strength for values around 0.01 oersted. This shows that for sufficiently small fields ordinary hysteresis is absent at 200 Mc so that all our results refer to *reversible* magnetization processes. In fact, the trend of the data of Kreielsheimer[19] indicates that even for fields of several oersteds, ordinary hysteresis is no longer present at 200 Mc.

The static (or low frequency) magnetization, however, is subject to ordinary hysteresis with respect to the polarizing field H_0. For this reason, the R.F. permeability is a double valued function of H_0 if the latter, instead of being applied in pulses starting from a uniquely magnetized state (as in Section III), is applied cyclically to the magnetic specimen. It is this dependence that will be referred to as "hysteresis effect" throughout the present paper. The double valued function mentioned above has the form of the "butterfly" curve which will be discussed later. This curve represents the combined effect of those reversible processes which are still effective at 200 Mc; the independent variable is essentially the state of static magnetization of the specimen.

Hysteresis effects of this kind can be rapidly examined in relatively small polarizing fields by using a direct or low frequency current through the center conductor and measuring the high frequency transmission of the cavity as a function of cyclic polarization. Although this method yields only the apparent permeability μ_R[20] rather than μ_1 and μ_2, it does have the advantage of not requiring the complicated pulse technique which was developed primarily for the accurate measurement of resonance frequency changes. On the typical "butterfly" curve shown in Fig. 5,

[18] V. E. Legg, Bell Sys. Tech. J. **18**, 438 (1939).

[19] See reference 1, pp. 234–237.

[20] As shown in Appendix IV, $\mu_R=|\mu|+\mu_2$.

the voltage transmission of the cavity, as determined by the rectified current output of the receiver, is plotted against the polarizing current in amperes. The dielectric bead, which is adjusted to resonate the cavity at $H_0=0$, remains fixed throughout the experiment.

To interpret the butterfly curves we use an equation similar to (24) and obtain

$$(V_0/V)^2=(V_0'/V')^2[1+4Q^2(\delta'-\Delta\nu)^2/(\nu+\delta')^2]\times[1+4Q_0^2(\Delta\nu/\nu)^2]^{-1}, \quad (28)$$

where the subscript zero refers to the demagnetized state ($H_0=0$) and δ' is the change in resonance frequency corresponding to a change in polarizing field from zero to H_0. Since $V_0'/V'=Q_0/Q$, $\delta'\ll\nu$, and $\Delta\nu=0$, Eq. (28) becomes

$$(V_0/V)^2=(Q_0/Q)^2[1+(\delta'/W')^2], \quad (29)$$

where $2W'=\nu/Q$ is the width, at the half-power point, of the resonance curve corresponding to a polarizing field H_0. From the measurements of δ *versus* H_0 we know that $\delta'\ll W'$ for all but very high fields. In the case of magnetic iron, for example, the maximum value of δ, which is almost as large as δ', is about 80 kc, whereas the corresponding W' is about 167 kc ($\nu=2\times10^5$, $Q=600$), so that $(\delta'/W')^2$ never exceeds 0.23. Thus, we may use

$$V_0/V=Q_0/Q \quad (30)$$

instead of Eq. (29) for low and intermediate H_0.

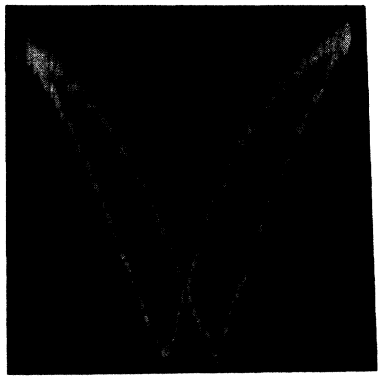

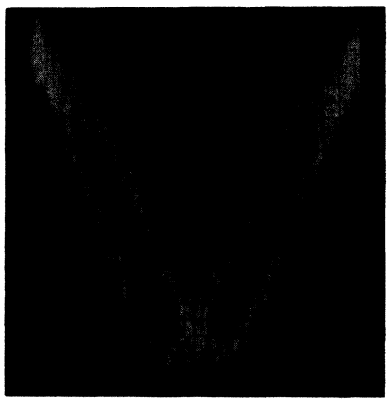

FIGS. 6 and 7. Oscillograms of butterfly curves for magnetic iron at 200 Mc (Fig. 6), and at 975 Mc (Fig. 7), using a 60-c.p.s. polarizing field of 17.7-oersted amplitude. The ordinates represent the modulated part of the cavity transmission and the abscissae are proportional to the polarizing field. The noise signals appearing in Fig. 7 are a result of the larger gain used at 975 Mc, where the dependence of the permeability on a polarizing field is less pronounced than at 200 Mc.

If the inner conductor of the cavity consisted completely of the magnetic material under investigation, and if the rest of the cavity had infinite conductivity in addition to being non-magnetic, then the measured Q's, and hence the ordinates of the butterfly curve, would be inversely proportional to the corresponding α's and to the square root of the apparent permeabilities.[21]

In the actual case of an imperfect cavity with a partially magnetic inner conductor, we have, analogously to Eqs. (15) and (17),

$$\alpha_0-\alpha=(1/2\gamma)(1/Q_0-1/Q),$$

which may be rewritten by using Eq. (30) to yield

$$(\alpha_0-\alpha)/\alpha_0=(1/2\gamma Q_0\alpha_0)(V-V_0)/V=\mathfrak{N}, \quad (31)$$

where the measurable quantity $\mathfrak{N}$ equals[21] the fractional change of the square root of the apparent permeability as the polarizing field is changed from zero to some value H_0.

From Eq. (31) we obtain[21] the expression

$$\mu_R/(\mu_R)_0=(1-\mathfrak{N})^2, \quad (32)$$

used for the interpretation (Table II, Section V) of the butterfly curves. To determine $\mathfrak{N}$ and to find the actual value of $(\mu_R)_0$ the quantity α_0 must be measured. This is accomplished with a fair degree of accuracy ($\leq$15 percent) by actually substituting a brass inner conductor for the partially magnetic inner conductor. Simple Q measurements may then be used (without pulsing)

[21] As shown in Appendix IV, $\alpha/\alpha_\infty=(\mu_R)^{\frac{1}{2}}$.

to obtain α_0 from the equation

$$\alpha_0-\alpha_{Br}=(1/2\gamma Q_{Br})[(Q_{Br}/Q_0)-1], \quad (33)$$

where the subscript Br refers to brass. The attenuation α_{Br} is calculated from Eq. (19) by using ρ_{Br} in place of ρ.

The butterfly curve shown in Fig. 5 was taken on 4–79 Mo Permalloy (at 200 Mc) by using a continuous direct current to generate the polarizing field. Starting from the demagnetized state, marked "A," the dashed line corresponds to the initial magnetization curve and merges into the butterfly curve (solid line) when the cyclic state is reached. The slight unsymmetry of the curve is due to heating effects caused by the application of the polarizing current for a relatively long time. These effects may be avoided by using a polarizing current of low audiofrequency and displaying the rectified cavity output on an oscilloscope where the butterfly curve may be photographed. The curve corresponding to the initial curve, of course, does not appear when an alternating polarizing field is used. Figures 6 and 7, taken on magnetic iron at 200 and 975 Mc, respectively, provide examples of such photographs. A further refinement is introduced by "chopping" the receiver output by means of an electronic switch. This method allows the zero level of the cavity transmission to be included in the photograph as a horizontal straight line that can be used for reference purposes. The typical example of Fig. 8 shows this type of presentation for 4–79 Mo Permalloy (at 200 Mc) where the permeability, and consequently the modulation of the cavity output, are relatively large, so that details of the butterfly curve are discernible. In those cases where the modulation is small compared to V_0, the cavity transmission for $H_0=0$, the determination of $\mathfrak{N}$ requires a scope calibration. The latter involves measuring the number of divisions on the screen of the cathode-ray tube which would be equivalent to V_0 if the gain were equal to that used in connection with the butterfly photograph.

The general results of the butterfly investigations may be summarized as follows:

(1) As expected, the shape and size of the butterfly curves is independent of the frequency of the polarizing field. Experiments in support of this statement were carried out on the same specimen at frequencies of zero, 60, 400, and 800 cycles/sec.

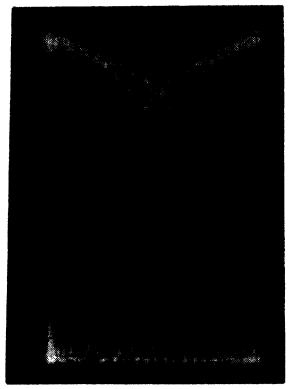

FIG. 8. Oscillogram of a typical butterfly curve (4–79 Mo Permalloy at 200 Mc) obtained by using an electronic switch; the ordinates represent the total cavity transmission.

(2) The butterfly curves do depend, to a small extent, on the maximum value of the polarizing field that is used in traversing the hysteresis cycle.

(3) There seems to be a superficial resemblance between our butterfly curves and the butterfly curves obtained by plotting the incremental static[22] permeability as a function of a polarizing field. In detail, however, these two types of curves differ in two important respects:

(*a*) As the polarizing field is changed from zero to several oersteds, the apparent high frequency permeability, as computed from the butterfly curve, changes by a much smaller fraction than the incremental static permeability.

(*b*) The positions of the minima on the high frequency butterfly curve, which correspond to a maximum apparent permeability, often occur at larger values of H_0 than those on the static curve for the same substance.

Numerical data (Table II) on the statements "*a*" and "*b*," as well as their interpretation, are given in Section V.

V. RESULTS AND DISCUSSION

As the penetration depth of a 200-Mc electromagnetic wave in iron or permalloy is less than 10^{-3} cm, the measured permeabilities are surface properties of the metal under investigation. In any interpretation of the data consideration must therefore be given to the effect of surface conditions on the processes of magnetization as well as to the response of these processes to high frequency excitation. Static measurements deter-

[22] G. W. Elmen, Bell Sys. Tech. J. **15**, 113 (1936), published such curves for several magnetic substances. The frequency of the small alternating field was 200 cycles/sec., and its amplitude was of the order of 0.001 oersted. Presumably, however, the results would have been the same if a static incremental field had been used.

mine the magnetization in the interior of the metal and give some indication of the processes of magnetization taking place at various points on the magnetization curve. Consequently, when made on the same sample of metal as the high frequency measurements, they are an invaluable aid in disentangling the different effects.

Our results for magnetic iron at 200 Mc and 975 Mc are shown in Fig. 9. Curves are given for the in-phase and out-of-phase components of the permeability, μ_1 and μ_2, the static incremental permeability, μ_{stat}, and the loss tangent of the susceptibility, $\mu_2/(\mu_1-1)$. The latter are the two topmost curves whose ordinate scale is on the right-hand side of the figure.

The most striking feature of our experimental results is the equality of μ_{stat} and μ_1 at both frequencies for all values of the polarizing field, H_0, greater than 50 oersteds. It is evident from Fig. 10, in which a typical[23] magnetization curve for magnetic iron is shown, that these fields are well beyond the knee of the magnetization curve. Consequently, we may conclude that the processes giving rise to changes in magnetization close to saturation respond fully (only weakly damped) to the high frequency excitation and that they differ in no way on the surface and in the interior of the samples we used.

The process known to be present, and usually assumed to be wholly responsible for magnetization changes close to saturation, is termed domain or spin rotation. According to this conception,[1] developed by Akulov and Gans, the metal is divided into domains in which the spins of the individual ions are ridigly coupled by the Heisenberg exchange force so that each domain is magnetized to saturation. The direction of the domain spin is fixed by the balance between the torque of the applied field and the torque from the anisotropy in the crystalline field. Changes in

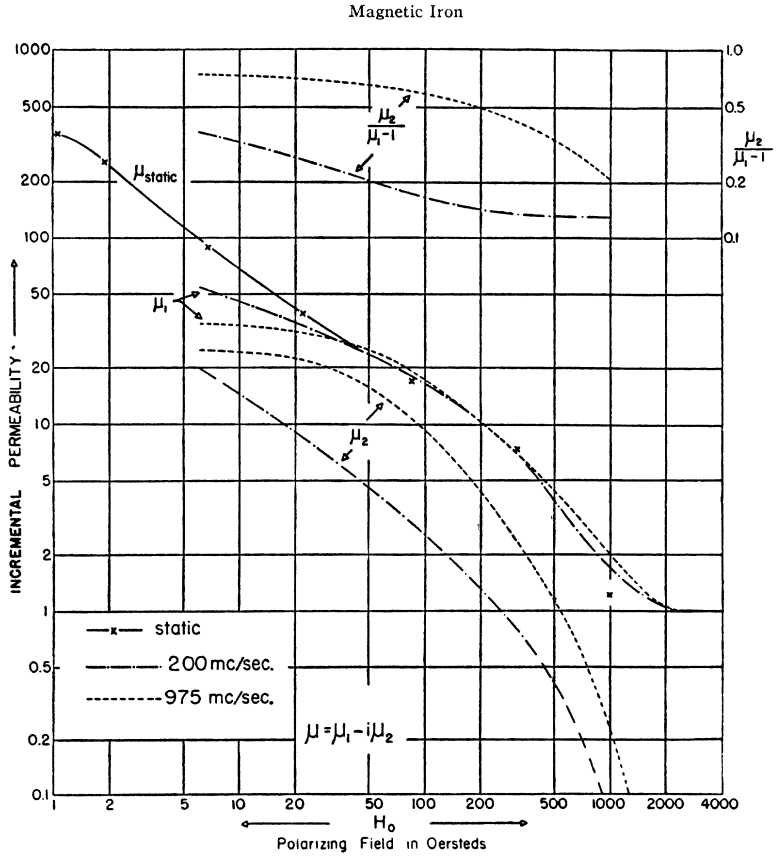

FIG. 9. Experimental permeabilities as a function of the polarizing field H_0 for magnetic iron at 0, 200, and 975 Mc.

[23] The typical magnetization curves of Figure 10 were taken from Legg's paper (see reference 18).

magnetization are produced by disturbing this balance when the applied field is altered. Saturation occurs when the torque of the applied field is so large that the crystalline field has a negligible influence on the direction of the domain spin.

The fact that $\mu_1=\mu_{stat}$ implies that domain rotation, at least for $H_0>50$ oersteds, responds fully to 975-Mc excitation. If the penetration depth of the 975-Mc field were smaller than the domain size, this would not be possible. The torque exerted on the spin would then be smaller, and since the rigid spin coupling causes the whole domain to rotate, the induced magnetization in the region of the applied field would be diminished. As the experimental result shows that the response is not diminished, and as the penetration depth of a 975-Mc wave in iron for $\mu=25$ is 1.0×10^{-4} cm, we can conclude[24] that the domains whose spins rotate are smaller than 10^{-4} cm for polarizing fields between 50 and 500 oersteds. It should be noted that the entire volume in which the high frequency field exists must be partitioned by domains to this size. If this were not so, the contribution to μ_{stat} of spin rotation, which takes place throughout the metal, would be larger than to μ_1.

The question arises as to whether 10^{-4} cm is the largest possible domain size. Recent experiments on the depolarization of slow neutrons[25] by the magnetic discontinuities in iron in a field of 10,000 oersteds have shown that the ultimate domain size is certainly greater than 7×10^{-4} cm and is probably the size of the microcrystal itself. Microphotographs of the samples used in the present experiments show a grain size[26] of 1.4×10^{-2} cm$\pm$20 percent. Consequently, the ultimate domain size in our samples is at least a hundred times the limit (10^{-4} cm) set above.

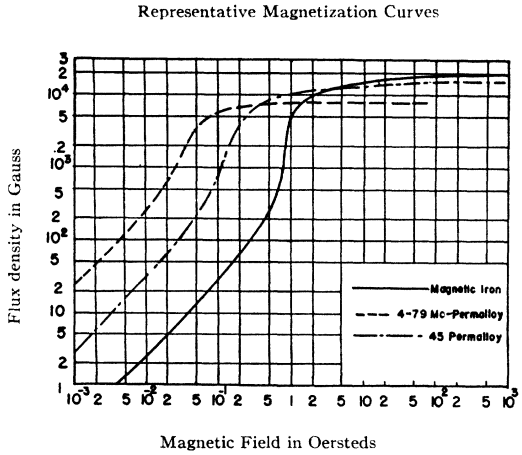

FIG. 10. Typical magnetization curves (reproduced from Leggs' (see reference 18) paper) for magnetic iron, 4–79 Mo Permalloy and 45 Permalloy.

The fact of a larger domain size at fields above 500 oersteds means that the domains existing in fields below 500 oersteds (which must be smaller than the skin depth for $\mu=4$, and thus smaller than 2.5×10^{-4} cm) are not stable, and that in higher polarizing fields they coalesce to form the larger domains. Therefore, above 500 oersteds wall displacements still occur and must contribute to changes in magnetization. We are, therefore, led to the idea of domains that are far more stable than those commonly supposed to exist at low fields and to disppear at the knee of the magnetization curve. It is most unlikely that wall displacements should contribute to magnetization above 500 oersteds and not below it. Consequently in the region $50<H_0<500$ oersteds wall displacements should also be contributing to the magnetization.

The existence of wall displacements for $H_0>50$ oersteds is confirmed by the quantitative results of the spin rotation theory. According to Gans'[27] formulae, which give the permeability in terms of the applied field, the saturation moment per unit volume, and the anisotropy constant, the permeability from spin rotation in zero field for polycrystalline iron is 14. As μ_1 (or μ_{stat}) is not reduced to this value until a polarizing field of 140 oersteds is applied, the actual permeability

[24] This is contrary to the assumption used by C. Kittel, Phys. Rev. **70**, 281 (1946), who attributed the decrease of the permeability at high frequencies to the smallness of the skin depth compared to the domain size. (The Barkhausen effect leads to estimates (see reference 1) of domain dimensions ranging from 10^{-3} to 10^{-4} cm.)

[25] D. J. Hughes, J. R. Wallace, and R. H. Holtzman, Phys. Rev. **73**, 1277 (1948). See also O. Halpern and T. Holstein, Phys. Rev. **59**, 960 (1941) and F. Bloch, M. Hammermesh, and H. H. Staub, Phys. Rev. **64**, 47 (1943).

[26] Even if iron oxide occlusions, clearly visible in the microphotographs, should determine the ultimate domain size, it would be greater than 3×10^{-3} cm. This seems a very unlikely possibility because such occlusions must have been present in the iron used in the neutron experiments and furthermore the hydrogen annealing had reduced most of the oxygen in the surface of our samples.

[27] R. Gans, Ann. d. Physik **15**, 28 (1932).

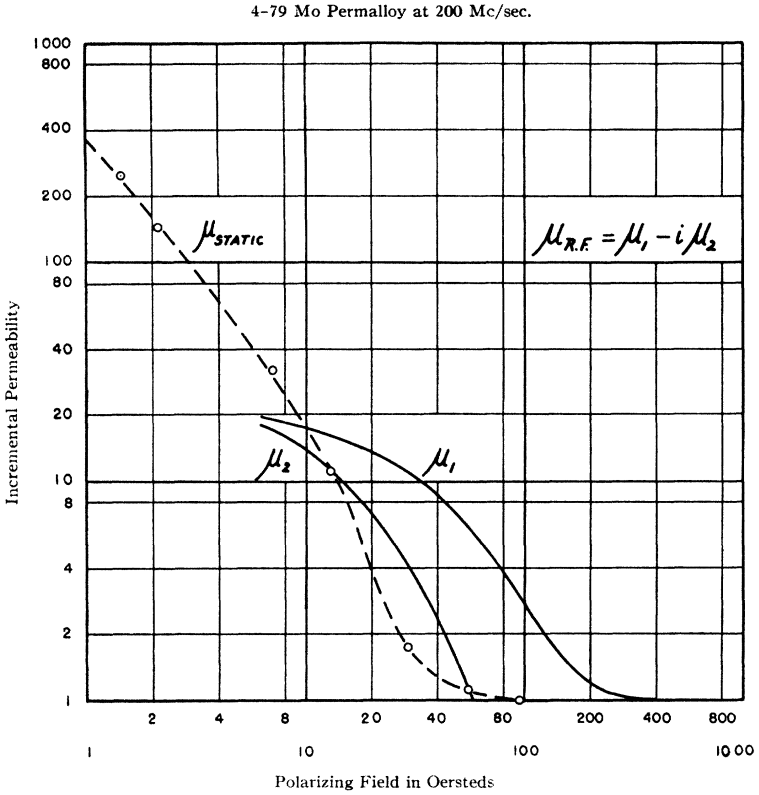

FIG. 11. Experimental permeabilities as a function of the polarizing field H_0 for 4–79 Mo Permalloy at 0 and 200 Mc.

exceeds[28,29] the calculated value by a large amount throughout this region. Since the conditions for the applicability of Gans' theory are well satisfied in our samples, this excess in the permeability can be attributed to changes in magnetization by wall displacements.

Let us next consider how the "50-oersted processes" of magnetization may behave at lower fields. The domains involved certainly cannot become larger; hence the contribution of spin rotation should still be present in accordance with Gans' formula. The domain walls, however, must contribute much more in order to account for the high values of μ_{stat} at low fields. This may occur either because of the motion of additional walls obtained by subdivision of the 50-oersted domains (the notation H_0-domain is used to designate a domain that exists in a field of H_0 oersteds) or because of the increased mobility and perhaps increased length of 50-oersted domain walls at lower fields. The first alternative means that magnetization (at any frequency) in lower fields occurs not only by processes active in higher fields but also by *additional processes* which come into being at the lower fields. The second alternative means that the larger magnetization changes in lower fields are the results of *altered characteristics* in the process active at higher fields.

The damping forces on domain walls are presumably the result of eddy currents induced by the change in magnetization when the walls are displaced. While the damping forces depend on the velocity of the wall, they do not depend directly on the polarizing field or on the stability

[28] H. Lawton and K. H. Stewart, Proc. Roy. Soc. **A193**, 72 (1948), have calculated magnetization curves for iron single crystals of simple shape for the case where the field is applied in an arbitrary direction with respect to the crystal axes. Their theory (which takes into account demagnetization effects on the surface of the sample) is based on spin rotation and the results are in good agreement with experiment down to relatively small fields. It therefore appears that the magnetic behaviour of polycrystals and single crystals is fundamentally different.

[29] It may be noted that microscopic observations of magnetic powder patterns on unstrained surfaces of single crystals indicate magnetic inhomogeneities of about 10^{-2} cm. See H. J. Williams, Phys. Rev. **70**, 106 (A) (1946); also **71**, 646 (1947); **72**, 529 (A) (1947); **73**, 1246 (A) (1948). If magnetic structures smaller than 10^{-4} cm existed in a single crystal, they could not be detected with the resolving power of a microscope utilizing visible light.

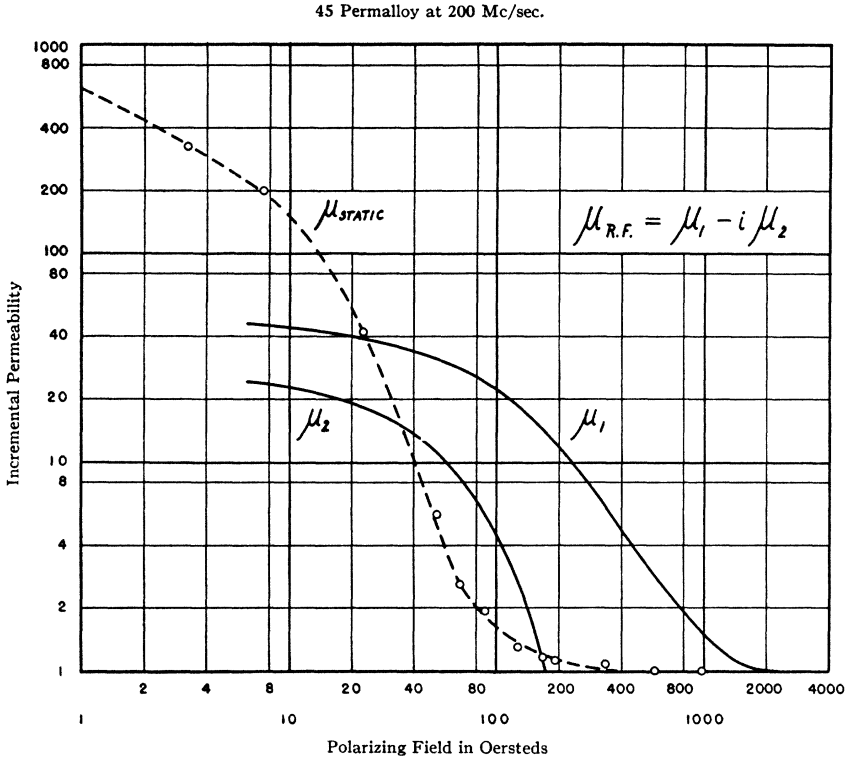

FIG. 12. Experimental permeabilities as a function of the polarizing field H_0 for 45 Permalloy at 0 and 200 Mc.

of the wall. On the other hand, the restoring force should be larger for the domain walls in higher fields because only the domains of greater stability exist in the higher fields. It is thus easily shown[30] that the induced magnetization, and hence $\mu-1$, has the form

$$\mu-1=(\mu_{\text{stat}}-1)(1-i\omega\tau)(1+\omega^2\tau^2)^{-1}, \quad (34)$$

where τ is a relaxation time that is smaller for the more stable domains. When the walls are highly damped, $\omega\tau\gg1$, and the out-of-phase component of magnetization, μ_2, is much larger than the in-phase component, μ_1-1.

Examination of Fig. 9 shows that μ_{stat} increases by a factor of four in passing from 6.25 oersteds to zero fields. Since μ_1 at 200 Mc is but a fifth of μ_{stat} at $H_0=0$, these weak-field domain walls must be highly damped[31] and do not contribute to μ_1. Furthermore, nothing like the fourfold increase in μ_{stat} is reflected in μ_2 so that the contribution of weak-field domain walls to μ_2 must also be small. As H_0 is reduced from 6.25 oersteds to zero, the increase in μ_2 amounts to about 18.[32] This figure sets an upper limit on the contribution of weak-field domain wall displacements to μ_2. Since $\mu_{\text{stat}}\approx360$ at $H_0=0$, Eq. (34) gives $\omega\tau\geq20$ at 200 Mc so that weak-field wall

[30] R. Becker, see reference 1, pp. 237–242. The general reasoning given by Becker may be applied individually to the walls of all the domains characterized by a given degree of stability. All such walls have a relaxation time which depends on the degree of domain stability; their displacements contribute a portion (according to their number) to the total static and high frequency susceptibility.

[31] The extinction of wall displacements mentioned in paper I refers to the weak-field domains.

[32] Our permeability data for $H_0<6.25$ oersteds (not shown in Figs. 9, 11, and 12) are uncertain because of the hysteresis effect, and only approximate values can be given for the permeability at $H_0=0$. These are $\mu_1=78$ and $\mu_2=38$ at 200 Mc, and $\mu_1=36$ and $\mu_2=25$ at 975 Mc. To compare these results with those given in the literature we note that C. Kittel, Phys. Rev. **70**, 281 (1946), has summarized the experimental values of the apparent permeabilities μ_R and μ_L of "iron" and drawn a smooth curve through the most reliable data. Using this experimental curve, and the equations of Appendix IV, we find $\mu_1=80$ and $\mu_2=39$ at 200 Mc, and $\mu_1=\mu_2=34$ at 975 Mc. The good agreement between the two sets of data is largely accidental because the mean values derived from previous measurements refer to different materials (even in the case of μ_R and μ_L at the same frequency) and are subject to considerable variations. This statement is supported by recent results of G. Eichholz and G. F. Hodsman, Nature **160**, 302 (1947), on the apparent permeability μ_R in various types of iron and steel. A comprehensive review of past work on apparent permeabilities at high frequencies was given by J. T. Allanson, J. Inst. Elec. Eng. **92**, Part III, 247 (1945).

displacements must show considerable damping ($\omega\tau \approx 1$) at some frequency below 10 Mc.

The extinction of weak-field domain wall displacements implies that the *first* of the two alternatives above is correct, and the high frequency magnetization in weak fields arises almost entirely from strong and intermediate-field domain walls (and spin rotation). The character of these processes remains sensibly unchanged at the lower fields. This is most clearly shown by the behavior at 975 Mc where both μ_1 and μ_2 are nearly constant below 50 oersteds; spin rotation accounts for the slight increase in μ_1. According to our view 50-oersted domain walls and spin rotation are responsible for the entire permeability at 975 Mc below 50 oersteds. At this frequency μ_1 in intermediate fields is smaller than at 200 Mc, and this fact indicates that the 6- to 50-oersted domain wall displacements have been damped out at 975 Mc. The decrease of the loss tangent at 200 Mc from 10 to 50 oersteds is explained naturally by the disappearance of the intermediate-field domains whose wall displacements are more damped.

One difficulty occurs in the use of Eq. (34). The loss tangent of 0.65 at 50 oersteds for the 975-Mc permeability implies that μ_1 should be about 30 percent smaller than μ_{stat}, a discrepancy which is definitely outside the experimental error.[33] Consequently there is some doubt as to the meaning of the experimental values of μ_2 or as to the applicability of Eq. (34). There are some indications (which will be reported in a later paper) that the experimental values of μ_2 depend on surface conditions much more sensitively than those of μ_1.

Our results for 4–79 Mo Permalloy (4-percent Mo, 79-percent Ni) and for 45 Permalloy (45-percent Ni) are shown in Figs. 11 and 12. As in the case of magnetic iron, relatively small damping is indicated at high polarizing fields. Contrary to the situation in iron, μ_1 becomes larger than μ_{stat} and higher values of H_0 are required to reduce μ_1 to unity than to produce static saturation. As the possibility of resonance is excluded by the behavior of μ_2, the surface layer of Permalloy behaves like a "harder" magnetic substance than the interior. This is probably not the effect of a demagnetizing factor from surface scratches, which, on microscopic examination, appear no more pronounced in the permalloy than in the iron samples. It could result from stresses in the surface because the magnetic properties of Permalloy are much more sensitive to stresses than those of iron. To understand such effects a comprehensive investigation of surface conditions has been undertaken, a part of which has appeared.[34] Whatever the effect, it could undoubtedly change the weak-field domain wall displacements in Permalloy. However, the complete extinction of the large changes in μ_{stat} when H_0 is less than 0.5 oersted indicates strongly that these displacements are highly damped in Permalloy also.

So far we have not discussed the irreversible wall displacements that take place when one domain configuration changes to another configuration of lower energy, which is not obtained from the first by infinitesimal displacements. The high frequency changes in magnetization are necessarily reversible (see Section IV). Nevertheless, the response depends on the domain configurations and will reflect changes in these configurations whether they are reversible or irreversible. This is clearly demonstrated by the results of the technique described in Section IV which are summarized in Table II.

In general the hysteresis effects shown in the oscillograms of Figs. 6, 7, and 8 are smaller at 200 Mc and much smaller at 975 Mc than might be expected from the corresponding changes in static fields. This is illustrated in columns V and VI of Table II in which the permeability at zero field in the remanent[35] state is compared to the permeability in a polarizing field of 18 oersteds and to the maximum permeability reached in the

[33] The error in μ_1 is estimated as less than ± 5 percent but the values of μ_2 are considerably less certain. Since μ_2 depends on the small difference $\alpha - \beta$ (Eq. 22), it is difficult to determine at fields close to saturation. This is especially true in iron, where δ_∞ could not be measured directly and was found by an extrapolation (as in Fig. 4) that is subject to an error of about ± 2 percent. Nevertheless, the error in μ_2 is estimated as less than ± 10 percent for small values of H_0 and as less than ± 50 percent at $H_0 = 500$ oersteds.

[34] G. T. Rado, M. Maloof, and H. Rosenblatt, Phys. Rev. **74**, 1206 (A) (1948).

[35] The effects indicated by these comparisons would appear more pronounced had the ratios in columns V and VI of Table II referred to the demagnetized state rather than to the remanent state.

hysteresis cycle. This result follows at once from the extinction by damping of the weak-field domain wall displacements which contribute most to the static changes in magnetization at low fields.

Inspection of column III of Table II shows that the maximum permeability in the hysteresis cycle occurs at a higher polarizing field for higher frequencies. As the changes in permeability in low fields at 200 Mc are mostly wall displacements of the 6- to 50-oersted domains, the coercive force for these domains is greater, as might be expected from their greater stability, than it is for the weak-field domains. Similarly at 975 Mc the wall displacements of 50-oersted domains give a still greater coercive force.

Another interesting feature of the results is that the hysteresis loops indicated by the high frequency measurements (butterfly curves) are wider than the corresponding static ones. Since at 975 Mc the permeability changes are due to the most stable domains, the ratio of high field hysteresis changes to low field hysteresis changes will be greatest for 975 Mc in accordance with observation. Indeed the existence of wall displacements at 500 oersteds implies that irreversible changes can take place in this strong a field.

The absence of any hysteresis effects reflecting irreversible changes in weak-field domains requires an explanation when it is remembered that we have already indicated why spin rotation in these domains must contribute a considerable fraction of the high frequency permeability. Of course at low frequencies the relative contribution of spin rotation to the weak field permeability is very small. Since the induced magnetization in spin rotation depends on the magnitude of the angle between the spin direction and the applied field, an irreversible change that alters this angle will be reflected in the spin rotation permeability. However, if the irreversible displacement is simply a reversal in sign of the spin direction ("180-degree wall") along the crystal axis, there will be no change in spin rotation permeability. It seems plausible that the irreversible changes occurring when the direction of the applied field is reversed are of this kind and should be the predominant type for weak-field domain hysteresis.

APPENDIX

I. Theory of the γ-Factor

In this appendix we calculate the change of the propagation constant (or refractive index) in a coaxial cavity resulting from a replacement of a *section* of the inner conductor by a similar section which differs in its conductivity and/or permeability from the original section. The result applies if one metal (A) is replaced by another metal (B), as in the substitution method of Section IV, or if the electromagnetic properties of a given metal are altered by a static magnetic field (Section II) or other means. For the purpose of this calculation we may assume, without loss of generality, that the outer conductor and end plates of the cavity are perfect conductors and non-magnetic.

The refractive index ($n=k/k_0$) is given by $n_A=1-i\alpha_A+\beta_A$ and its deviation from unity is now due to the inner conductor only. If the whole inner conductor (A) were replaced by another metal (B), the change of the refractive index would be $\Delta n=-i(\alpha_B-\alpha_A)+(\beta_B-\beta_A)$, but if only a section of the inner conductor is replaced, the value of Δn must be modified as shown below.

The cavity may be divided into three sections according to the properties of the inner conductor. In Sections I ($z=0$ to $z=z_1$) and III ($z=z_2$ to $z=z_3\approx\lambda_0/2$) the inner conductor consists of metal A, and in the intermediate Section II ($z=z_1$ to $z=z_2$) it is made of metal B. As the tangential components E_r and H of the field must be continuous at the boundaries (z_1 and z_2), the impedance $Z=E_r/H$ must also be continuous, and the solution of the boundary value problem may be carried out in terms of Z. Since $Z=-n$ in a coaxial line (Eqs. (1) and (2)), the expression

$$Z_m=n_m(e^{\theta}-c_m'e^{-\theta})(e^{\theta}+c_m'e^{-\theta})^{-1}$$

is consistent with the field equations and describes the reflection of the waves in the cavity. Here θ is an abbreviation for in_mk_0z, the reflection coefficients c_m' are undetermined constants, and the subscript m ($m=$I, II, III) identifies the three sections of the cavity. Writing the constants in exponential form ($c_m'=\exp(-2c_m)$) the expression for Z_m is equivalent to

$$Z_m=n_m\tanh(in_mk_0z+c_m).$$

The value of the refractive index in the various sections of the cavity is given by $n_{\rm I}=n_{\rm III}=n_A$ and $n_{\rm II}=n_B=n_A+\Delta n$. Since $c_{\rm I}'=1$ (E_r vanishes at $z=0$), $c_{\rm I}=0$, and only the two constants $c_{\rm II}$ and $c_{\rm III}$ are unknown. These constants may be evaluated from the two equations resulting from the boundary conditions $Z_{\rm I}=Z_{\rm II}$ at z_1, and $Z_{\rm II}=Z_{\rm III}$ at z_2. The calculation is based on the same approximation ($k-k_0\ll k_0$, or $n-1\ll1$) which was used in Section II, and the result shows that both $c_{\rm II}$ and $c_{\rm III}$ may be treated as small quantities of the order of Δn ($\Delta n\ll1$). It is convenient to introduce the quantity γ defined by

$$\gamma=(1/\pi)[k_0L+(2\sin^2k_0D-1)\sin k_0L], \qquad \text{(A-1)}$$

where $L=z_2-z_1$ is the length of the replaced section (metal B) and $D=|\lambda_0/4-(z_1+z_2)/2|$ is the distance of its center from the center of the resonator. Using this

abbreviation, we obtain $c_{III}=i\pi\gamma\Delta n$, and the value of Z_{III} at the end of the cavity ($z=z_3\approx\lambda_0/2$) is thus given by $n_A\tanh[i\pi(n_A+\gamma\Delta n)]$. Since $\gamma=1$ if the whole inner conductor is replaced ($L\approx\lambda_0/2$), the result of the calculation is that the change of the refractive index due to a replacement of a *section* of the inner conductor is given by $\gamma\Delta n$.

The foregoing calculation neglects the end-effects existing at z_1 and z_2; if L is sufficiently large, however, these effects may be shown to be negligible. Measurements of the cavity Q for several positions D of a given magnetic rod permitted several independent determinations of the attenuation α_0. Since these determinations made use of Eq. (33), which contains γ, the observed agreement (within the experimental error) of the various values of α_0 constitutes an experimental verification of the formula (A-1) for γ. In this connection we note that D must be measured from the electrical center of the cavity rather than from the mechanical center. The electrical center was found experimentally by determining the position corresponding to maximum Q on a symmetrical curve of cavity Q *versus* position of the magnetic rod. Other experiments showed that at 200 Mc $L=17.75$ cm is sufficiently large, and $L=4$ cm too small, for the γ-formula to be applicable; for $L\geq 10$ cm, deviations caused by end-effects appear to be negligible. In all the 200 Mc measurements we used $L=17.75$ cm and obtained a convenient value for Q_{bias} ($Q_\infty/Q_{\text{bias}}\approx 2$) by adjusting the distance D.

II. Calculation of Q_∞

Let us compare a cavity with brass inner conductor and a similar cavity whose inner conductor consists of a section of magnetic material and two sections of brass, as described in Section II. In analogy with Eqs. (17) and (33) we have

$$(1/2)(1/Q_\infty-1/Q_{Br})=\gamma(\alpha_\infty-\alpha_{Br}). \qquad \text{(A-2)}$$

The difference in losses represented in Eq. (A-2) is *independent* of any attenuation in the outer conductor and end plates, as well as of unknown losses in the cavity. In calculating α_∞ and α_{Br}, which refer to the inner conductor, we use Eq. (19) with suitable values for the resistivity. Substituting the resulting expressions into Eq. (A-2), one obtains

$$1/Q_\infty=\gamma c(\rho^{\frac{1}{2}}-\rho_{Br}^{\frac{1}{2}})/4\pi\nu^{\frac{1}{2}}a\ln(b/a)+1/Q_{Br}, \qquad \text{(A-3)}$$

where the resistivities ρ (of the magnetic material) and ρ_{Br} (of brass) are in e.s.u. (seconds). Equation (A-3) allows the calculation of Q_∞ from the *measured* value (Q_{Br}) of the cavity Q with brass inner conductor. The resistivities are measured on the actual rods used for the inner conductor and the remaining quantities are determined by the dimensions of the cavity and the frequency.

III. Theory of the Dielectric Tuner

In considering the effect of the dielectric tuner on the resonant wave-length of the cavity, we may assume, without loss of generality, that the cavity has ideal walls. Thus the refractive index in the cavity is unity except in the region occupied by the dielectric bead; in this region $n=\epsilon_d^{\frac{1}{2}}$, where ϵ_d is the dielectric constant (assumed to be a real number) of the polystyrene bead. By solving a boundary value problem similar to that involved in the theory of the γ-factor, and assuming that the length L_d of the bead is small ($L_dk_0\ll 1$), one obtains the following expression for the increase of the resonant wave-length ($\Delta\lambda_0$) of the cavity as a result of the presence of the bead:

$$\Delta\lambda_0=2L_d(\epsilon_d-1)\sin^2k_0L_d', \qquad \text{(A-4)}$$

where L_d' is the distance of the bead from either end of the cavity. Equation (A-4) shows, in agreement with experiment, that the calibration of the cavity ($\Delta\lambda_0$ *versus* position of the bead) is sensibly linear over an appreciable part of the range between one end of the cavity ($L_d'=0$) and its center ($L_d'\approx\lambda_0/4$). Because of the effect of the bead, the electrical center of the cavity (Appendix I) is moved slightly from the mechanical center to that side of the cavity which contains the bead. The changes in the cavity Q caused by displacements of the low loss polystyrene bead are negligible.

IV. Significance of Apparent Permeabilities

Assuming that the permeability μ is *real*, Eqs. (6) and (19) lead to the relations $\alpha/\alpha_\infty=\mu^{\frac{1}{2}}$ and $\beta/\beta_\infty=\mu^{\frac{1}{2}}$, where $\alpha_\infty=\beta_\infty$ is the value of α (or β) if the permeability is unity. Since, in general, α and β are not equal, the assumption of a real μ is contrary to experimental facts. Contradictions of this kind are well known (see reference 1, pp. 233–237) and led to a distinction[1] between a *real* permeability, μ_R, determined from a resistance measurement, and a *real* permeability, μ_L, determined from a reactance measurement. As pointed out by Becker[1] and particularly by Kittel (Phys. Rev. **70**, 281 (1946)), however, these two types of measurements reveal different aspects of the same fundamental phenomena. Experimental data may be expressed either in terms of the two apparent permeabilities μ_R and μ_L ($\mu_R\neq\mu_L$), or in terms of the complex permeability employed in the theory of W. Arkadiew (Physik. Zeits. **14**, 928 (1913)).

In our experiment the measured attenuation is due to resistive losses and the measured change of phase velocity is due to reactive changes. Thus, the definition of the apparent permeabilities leads to

$$\alpha/\alpha_\infty=\mu_R^{\frac{1}{2}} \quad \text{and} \quad \beta/\beta_\infty=\mu_L^{\frac{1}{2}}. \qquad \text{(A-5)}$$

Substituting the relations (A-5) into Eqs. (21) and (22), we obtain

$$\mu_1=(\mu_R\mu_L)^{\frac{1}{2}}, \qquad \text{(A-6a)}$$

and

$$\mu_2=(1/2)(\mu_R-\mu_L). \qquad \text{(A-6b)}$$

Using $|\mu|=(\mu_1^2+\mu_2^2)^{\frac{1}{2}}$, these equations result in

$$\mu_R=|\mu|+\mu_2, \qquad \text{(A-7a)}$$

and

$$\mu_L=|\mu|-\mu_2. \qquad \text{(A-7b)}$$

Equations (A-6) and (A-7), first given by Arkadiew [Zeits. f. Physik **27**, 37 (1924)], relate the complex permeability to the apparent permeabilities and are valid whenever a strong skin effect occurs.

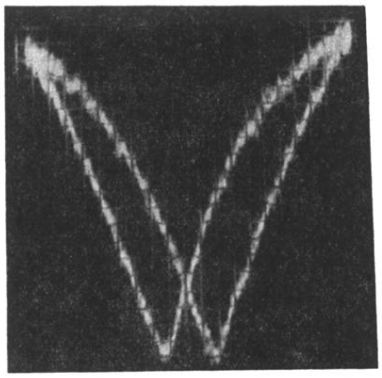

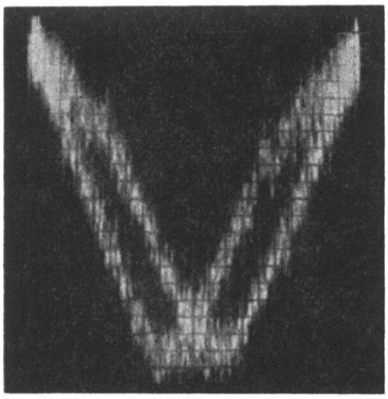

FIGS. 6 and 7. Oscillograms of butterfly curves for magnetic iron at 200 Mc (Fig. 6), and at 975 Mc (Fig. 7), using a 60-c.p.s. polarizing field of 17.7-oersted amplitude. The ordinates represent the modulated part of the cavity transmission and the abscissae are proportional to the polarizing field. The noise signals appearing in Fig. 7 are a result of the larger gain used at 975 Mc, where the dependence of the permeability on a polarizing field is less pronounced than at 200 Mc.

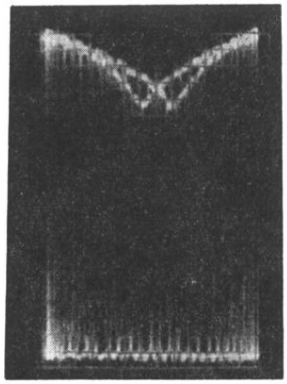

FIG. 8. Oscillogram of a typical butterfly curve (4–79 Mo Permalloy at 200 Mc) obtained by using an electronic switch; the ordinates represent the total cavity transmission.